



Title	Modeling Treatment Response for Lamin A/C Related Dilated Cardiomyopathy in Human Induced Pluripotent Stem Cells.
Author(s)	Lee, YK; Lau, VYM; Cai, Z; Lai, KWH; Wong, LY; Tse, HF; Ng, KM; Siu, DCW
Citation	Journal of the American Heart Association, 2017, v. 6 n. 8, p. e005677:1-36
Issued Date	2017
URL	http://hdl.handle.net/10722/246561
Rights	This work is licensed under a Creative Commons Attribution-NonCommercial-NoDerivatives 4.0 International License.

Modeling Treatment Response for Lamin A/C Related Dilated Cardiomyopathy in Human Induced Pluripotent Stem Cells

Yee-Ki Lee, PhD;* Yee-Man Lau, PhD;* Zhu-Jun Cai, MSc; Wing-Hon Lai, PhD; Lai-Yung Wong, BSc; Hung-Fat Tse, MD, PhD; Kwong-Man Ng, PhD; Chung-Wah Siu, MD

Background—Precision medicine is an emerging approach to disease treatment and prevention that takes into account individual variability in the environment, lifestyle, and genetic makeup of patients. Patient-specific human induced pluripotent stem cells hold promise to transform precision medicine into real-life clinical practice. Lamin A/C (LMNA)-related cardiomyopathy is the most common inherited cardiomyopathy in which a substantial proportion of mutations in the *LMNA* gene are of nonsense mutation. PTC124 induces translational read-through over the premature stop codon and restores production of the full-length proteins from the affected genes. In this study we generated human induced pluripotent stem cells-derived cardiomyocytes from patients who harbored different *LMNA* mutations (nonsense and frameshift) to evaluate the potential therapeutic effects of PTC124 in *LMNA*-related cardiomyopathy.

Methods and Results—We generated human induced pluripotent stem cells lines from 3 patients who carried distinctive mutations (R225X, Q354X, and T518fs) in the *LMNA* gene. The cardiomyocytes derived from these human induced pluripotent stem cells lines reproduced the pathophysiological hallmarks of *LMNA*-related cardiomyopathy. Interestingly, PTC124 treatment increased the production of full-length LMNA proteins in only the R225X mutant, not in other mutations. Functional evaluation experiments on the R225X mutant further demonstrated that PTC124 treatment not only reduced nuclear blebbing and electrical stress-induced apoptosis but also improved the excitation-contraction coupling of the affected cardiomyocytes.

Conclusions—Using cardiomyocytes derived from human induced pluripotent stem cells carrying different *LMNA* mutations, we demonstrated that the effect of PTC124 is codon selective. A premature stop codon UGA appeared to be most responsive to PTC124 treatment. (*J Am Heart Assoc.* 2017;6:e005677. DOI: 10.1161/JAHA.117.005677.)

Key Words: dilated cardiomyopathy • lamin A/C cardiomyopathy • nonsense mutation • PTC124 • translational read through

Lamins A and C (Lamin A/C) are intermediate filament proteins encoded by the autosomal *LMNA* gene and constitute major components of the nuclear lamina.¹ Mutations in *LMNA* cause a wide spectrum of human diseases collectively referred to as “laminopathies,”^{2–6} from multisystem involvement conditions such as Hutchinson Gilford progeria and muscular dystrophy to isolated dilated

cardiomyopathy. *LMNA*-related cardiomyopathy is characterized by early-onset atrioventricular block and atrial fibrillation and subsequently progresses to ventricular tachyarrhythmia with consequent sudden cardiac death, left ventricular dysfunction, and heart failure. *LMNA* mutations are the most common cause of familial dilated cardiomyopathy, accounting for 5% to 10% of all cases and up to 30% to 45% of families with dilated cardiomyopathy and conduction system disease.^{7,8} Despite a clear genetic basis, to date, no specific therapeutic strategies are available to modify the disease progression. In fact, the clinical management of *LMNA*-related dilated cardiomyopathy is no different from that for other forms of dilated cardiomyopathy. Genetically, *LMNA*-related cardiomyopathy is a dominant trait, and based on the results of mouse model, haploinsufficiency is likely the pathogenic mechanism.⁹ One important implication of nonsense mutations is a therapeutic possibility of alleviating or even reversing the disease process by translational read-through of premature stop codons and production of full-length proteins by interfering with ribosomal proofreading. For instance, PTC124, also known as ataluren, discovered through

From the Cardiology Division, Department of Medicine, Li Ka Shing Faculty of Medicine, The University of Hong Kong, Hong Kong SAR, China.

Accompanying Table S1 and Figures S1 and S2 are available at <http://jaha.ahajournals.org/content/6/8/e005677/DC1/embed/inline-supplementary-material-1.pdf>

*Dr Lee and Dr Lau contributed equally to this work.

Correspondence to: Chung-Wah Siu, MD, or Kwong-Man Ng, PhD, Cardiology Division, Department of Medicine, The University of Hong Kong, Queen Mary Hospital, Hong Kong, China. E-mails: cwdsiu@hku.hk; skymng@hku.hk
Received January 23, 2017; accepted May 2, 2017.

© 2017 The Authors. Published on behalf of the American Heart Association, Inc., by Wiley. This is an open access article under the terms of the Creative Commons Attribution-NonCommercial License, which permits use, distribution and reproduction in any medium, provided the original work is properly cited and is not used for commercial purposes.

Clinical Perspective

What Is New?

- This is the first study of the read-through drug PTC124 in patient human induced pluripotent stem cells-derived cardiomyocytes for treatment of nonsense (UGA stop codon-specific) related cardiac laminopathy by recovery of expression of full-length Lamin A/C.

What Are the Clinical Implications?

- This study demonstrates the potential feasibility of human induced pluripotent stem cells-based precision medicine approaches to predict clinical responses of dilated cardiomyopathy patients and to study disease mechanisms.
- Drug testing in patient human induced pluripotent stem cells-derived cardiomyocytes may be a possible approach to select PTC124 responders for entry into clinical trials.

high-throughput screening utilizing premature UGA luciferase reporters to promote read-through of the premature stop codon,¹⁰⁻¹² has been granted orphan drug designation by the Food and Drug Administration in the United States for the treatment of nonsense mutation-related genetic disease. A phase 3 clinical trial is ongoing to evaluate the clinical efficacy of PTC124 in patients with nonsense mutation cystic fibrosis, which accounts for around 10% of cystic fibrosis cases.¹³

Notwithstanding the cost, standard randomized, double-blind, placebo-controlled studies might not always be possible because the number of patients with the same condition harboring the same or similar mutation is usually small. Human induced pluripotent stem cells (hiPSC) generated from individual patients who harbor a specific mutation have been exploited to elucidate the pathogenic mechanisms of various cardiovascular diseases.¹⁴⁻¹⁹ The hiPSC technology is expected to revolutionize the concept of precision medicine by providing a steady supply of patient-specific functional cells for preclinical testing in order to identify the most effective and safest personalized strategies for a particular individual.²⁰ In fact, the US Food and Drug Administration has recently examined ways in which hiPSC-derived cardiomyocytes can be used in preclinical investigation of the potential risks in metabolic pathways or proarrhythmia events. Using hiPSC-derived cardiomyocytes generated from patients with *LMNA*-related cardiomyopathy, we have previously demonstrated that nuclear senescence and cell apoptosis are the key pathophysiological factors in *LMNA*-related cardiomyopathy.¹⁸ In the present study we generated iPSCs from 3 patients with documented *LMNA*-related cardiomyopathy arising from 2 different nonsense mutations (UGA and UAG) and a frame-shift mutation in the *LMNA* gene. We differentiated them into cardiomyocytes to evaluate the effects of

PTC124 on lamin A/C protein production, nuclear senescence, and cell apoptosis. Not only will our results allow us to differentiate a PTC124 responder from nonresponder to enter the clinical trials, but, more importantly, they demonstrate the feasibility of this iPSC-based precision medicine approach in studying genetic diseases.

Methods

Generation of hiPSC From Patients Carrying Cardiomyopathy-Associated *LMNA* Mutations

The study protocol for procurement of human tissue for the generation of hiPSCs was approved by the local Institutional Review Board and was registered at the Clinical Trial Center, the University of Hong Kong (IRB-UW08-258). After obtaining written informed consent from all participants, we collected skin biopsies. Skin biopsy samples were mechanically dissociated and plated onto 6-well culture dishes with the culture medium supplemented with 10% fetal bovine serum, as previously described.²¹ Dermal fibroblasts growing out from the skin tissue were expanded and transduced with lentiviruses encoding human OCT4, SOX2, KLF4, and c-MYC. Putative hiPSC clusters were typically observed at 14 to 21 days after lentiviral transduction and were manually dissected and expanded onto new matrigel-coated 6-well plates. The authenticity of the hiPSCs was confirmed with the expression of a panel of pluripotent markers, transgene silencing, OCT4 promoter demethylation, and teratoma formation after inoculation into severe combined immunodeficiency mice (data not shown). All stem cell characterization works have been reported previously.²¹

Cardiac Differentiation

Cardiac differentiation of hiPSCs was induced using a previously reported protocol.²² In brief, undifferentiated hiPSCs were maintained in mTeSR1 medium (STEMCELL Technologies Inc, Vancouver, BC, Canada). Four days before induction, hiPSCs were dissociated into single cells with accutase (Invitrogen, Carlsbad, CA) and then seeded onto a 12-well matrigel-coated plate (Thermo Scientific Inc, Waltham, MA) supplemented with Y27632 (5 μ mol/L) (Stemgent, Cambridge, MA). On the first induction day the culture medium was switched to RPMI medium (Life Technologies, Carlsbad, CA) without insulin and supplemented with B27 (Life Technologies) and a GSK- β inhibitor, CHIR99021 (12 μ mol/L) (Selleckchem, Houston, TX), and refreshed 24 hours later. On day 4, a Wnt signaling inhibitor, IWP2 (5 μ mol/L) (Selleckchem, Houston, TX), was added to the culture medium. Typically, spontaneously beating cardiomyocytes were

observed around 9 days after induction. The cells were maintained in the cardiomyocyte maintenance medium (RPMI medium with B27 supplement) and used in subsequent analyses.

LMNA-Related Cardiomyopathy Model

The hiPSC-based model of LMNA-related cardiomyopathy was induced using electrical stimulation according to our previously published protocol.¹⁸ Specifically, hiPSC-derived cardiomyocytes were seeded on 13-mm glass coverslips (Nunc A/S, Rockville, Denmark) and mounted on a 6-well plate filled with corresponding medium. Electrical stimulation was then delivered to the cultured cells for 4 hours with carbon electrodes using an 8-channel C-Pace cell culture stimulator (IonOptix Co, Milton, MA) at 6.6 V/cm, 1 Hz, 2 milliseconds with alternating polarity. The total number of cells was counted before and after electrical stimulation.²³⁻²⁵

PTC124 Treatment

A stock solution of PTC124 was prepared by dissolving the lyophilized PTC124 (Selleckchem, Houston, TX) in DMSO to a concentration of 10 mmol/L. The stock solution was diluted in cell culture medium and preheated to 37°C to ensure complete dissolution before being applied to the cells. To test the potential therapeutic effects of PTC124, hiPSC-derived cardiomyocytes were pretreated with PTC124 (50 μmol/L) for 7 days before electrical stressing.

Western Blot Analysis

Western blot analysis was performed following the protocol described previously.²⁶ In brief, cells of interest were washed with Dulbecco phosphate-buffered saline and lysed in RIPA buffer (Cell Signaling Technology, Danvers, MA) containing 0.2% Triton X-100, 5 mmol/L EDTA, 1 mmol/L PMSF, 10 μg/mL leupeptin, 10 μg/mL aprotinin with additional 100 mmol/L NaF and 2 mmol/L Na₃VO₄. The supernatant was collected after spinning for 20 minutes at 12 000g. The amount of protein was quantified using a Bio-Rad protein assay kit (Hercules, CA). For each sample, 50 μg of total protein was resolved on a 4% to 12% Bis-Tris plus gel (Gibco, Gaithersburg, MD) and transferred onto nitrocellulose membranes. After blocking with 5% nonfat dry milk in TBS (pH 7.4) with 0.5% Tween-20 at 4°C, the transferred protein was probed by primary mouse monoclonal antibodies specific to lamin A/C (clone 4C-11; 1:2000; Cell Signaling Technologies, Danvers, MA). As an endogenous control, the levels of β-actin were evaluated using a monoclonal antibody specific to β-actin. The location of the immunoreactive protein complex was detected with HRP-conjugated secondary antibodies (Cell Signaling

Technology, Danvers, MA; 1:2000) and visualized with standardized enhanced chemiluminescence systems.

Assessment of Nuclear Blebbing Events

At 30 to 40 days after induction of differentiation, hiPSC-derived cardiomyocytes were dissociated by collagenase treatment and subsequently seeded on gelatin-coated coverslips for immunostaining analysis and functional evaluation. For immunostaining, cells were fixed and permeabilized in 2% paraformaldehyde for 20 minutes at 4°C and then washed with wash buffer (Dulbecco phosphate-buffered saline with 0.1% Triton X-100; Sigma-Aldrich, St. Louis, MO). The nuclear lamina of hiPSC-derived cardiomyocytes was visualized by staining with antibodies specific to lamin A/C (clone 4C-11; 1:200; Cell Signaling Technologies, Danvers, MA) and cardiac-specific markers such as goat anti-tropoinin-T (1:400; Abcam, Cambridge, UK). Positively probed cells were visualized by addition of rabbit anti-goat IgG H+L Alexa 594 and rabbit anti-mouse IgG H+L Alexa 488 (Molecular Probes, Eugene, OR) for 30 minutes. Images were acquired using a fluorescence confocal Carl Zeiss LSM 700 microscope (Zeiss GmbH, Gottingen, Germany).

Terminal Deoxynucleotidyl Transferase dUTP Nick End Labeling Assay for Apoptosis

A terminal deoxynucleotidyl transferase dUTP nick end labeling (TUNEL) assay was performed using an in situ Cell Death Detection Kit, Fluorescein (Roche Applied Sciences, Mannheim, Germany) according to the manufacturer's protocol. Cells were grown on glass coverslips, fixed with 4% paraformaldehyde, and permeabilized with 0.1% Triton X-100 in 0.1% sodium citrate for 2 minutes on ice. Cells were incubated in TUNEL reaction mixture at 37°C for 60 minutes in a humidified dark chamber. The TUNEL-labeled samples were subjected to costaining with troponin-T antibodies for confirmation of cardiac identity. Coverslips were mounted onto glycerol-based mountant. Images were acquired using a Carl Zeiss fluorescence microscope with AxioVision 6.0 software (Zeiss GmbH, Gottingen, Germany). The number of apoptotic cells on electrical stimulation was further quantified using the APO-BrdU TUNEL Assay Kit (Molecular Probes, Inc, Eugene, OR). The dissociated cells were fixed in 1% (w/v) paraformaldehyde on ice for 15 minutes and then washed twice with Dulbecco phosphate-buffered saline at 300g for 5 minutes. The fixed cells were stored in ice-cold 70% (v/v) ethanol at -20°C before the nicked end labeling reaction. The cells were washed with wash buffer before incubation in TUNEL labeling solution for an hour at 37°C (10 μL reaction buffer, 0.75 μL TdT enzyme, 8 μL of BrdU, and 31.25 μL dH₂O). After further washing with rinse buffer, cells were

stained with the Alexa Fluor[®] 488 dye-labeled anti-BrdU antibodies for a half-hour. The propidium iodide/RNase A staining buffer was finally added to the cells before flow cytometry analysis. The positively labeled cells (green signal), a population with DNA fragmentation, were counted as percentage of apoptotic cells.

Taqman Assay for Quantification of LMNA Expression

Total RNA was extracted from fibroblasts using TRIZOL reagent following the procedure provided by the manufacturer (Life Technologies, Carlsbad, CA). For each sample, 1 µg of total RNA was used for cDNA synthesis using the QuantiTect Reverse Transcription kit (Qiagen, Venlo, The Netherlands). Taqman gene expression assay was carried out using a FAM-labeled probe derived from the Universal Probe Library (lamin A/C (*LMNA*): probe #66, troponin-T type 2 (*TNNT2*): probe #63 and α -tubulin (*TUB4q*): probe #75 (Roche Applied Sciences) in combination with FastStart Universal Probe Master (Rox) as the detection reagent (Roche Applied Sciences, Indianapolis, IN). The samples were analyzed as duplicates on the StepOnePlus real-time polymerase chain reaction system (Life Technologies). *TUBA4A* served as a housekeeping gene for normalization, and *TNNT2* was used for normalization of cardiac purity within the whole population.

Excitation-Contraction Coupling Analysis by Simultaneous Calcium Imaging and Video Edge Detection

To study the calcium-handling properties, hiPSC-derived cardiomyocytes were loaded with Fura-2 AM (Life Technologies, Carlsbad, CA), a calcium indicator, at a working concentration of 1 µM for 20 minutes. Unincorporated dye was removed, and the cells were subsequently incubated in Tyrode solution. For calcium transient measurements, field-stimulated electrical pacing was induced by the Myopacer EP Field Stimulator (IonOptix, Westwood, MA) at 40 V cm⁻¹, 5-millisecond pulse duration at frequencies of 0.5 Hz, 1 Hz,

1.5 Hz, and 2 Hz. The calcium fluorescence and video-edging (contractile force) signal were simultaneously recorded by MyoCam-S (IonOptix) using IonWizard 6.4 version 2 software (IonOptix). The acquisition rate of calcium imaging was 100 points/s. The Fura-2 required dual-wavelength excitation at 340 nm and 380 nm, and the emission signals were recorded at 505 nm. The calcium level was presented as a ratio of 340/380 nm ($F_{340/380}$) and calibrated with amount of free calcium (nmol/L). The calcium transients of every cardiomyocyte were recorded with background subtraction.

Statistical Analysis

Continuous variables are expressed as mean±SEM. Statistical comparisons between 2 groups were performed using Student t test or nonparametric Mann-Whitney test (for n<10). For analysis involving more than 2 groups, 1-way ANOVA analysis was used. For posttest, Tukey analysis was used to compare all pairs of columns. A *P* value <0.05 was considered statistically significant.

Results

Patient Characteristics, Generation of LMNA-Mutation-Harboring hiPSCs, and Cardiac Differentiation

Two patients with nonsense *LMNA* mutations and 1 patient with a frame-shift mutation were recruited to the study. The first patient was a 49-year old Chinese man who initially presented with atrial fibrillation and complete atrioventricular block and required permanent cardiac pacemaker implantation. Two years later, he developed sustained ventricular tachyarrhythmia and heart failure with an impaired left ventricular ejection fraction of 35%. An automatic implantable cardioverter defibrillator was therefore implanted (Table). His family history was remarkable for complete atrioventricular block and sudden cardiac death. Sequencing of the *LMNA* gene revealed a heterozygous single-base exchange (672G→T) in exon 4, resulting in an R225X nonsense mutation

Table. Cardiac Manifestations in Affected Subjects Bearing *LMNA* Mutations

<i>LMNA</i> Mutations	Sex	Cardiac Manifestations (Age of Manifestation)				
		Complete Heart Block	AF	VT/VF	Dilated Cardiomyopathy	AICD
R225X	M	+ (49)	+ (49)	+ (50)	+ (51)	+ (52)
Q354X	M	+ (50)	+ (50)	+ (56)	+ (50)	+ (50)
T518fs	M	+ (43)	+ (43)	+ (47)	+ (47)	+ (47)

AF indicates atrial fibrillation; AICD, automatic implantable cardioverter defibrillator; VT/VF, ventricular tachycardia/ventricular fibrillation. "+" represent presence of disease phenotype, while the ages of disease onset are shown the brackets.

(truncation in the coil 1B domain of both lamin A and C proteins), previously known to be associated with familial dilated cardiomyopathy^{18,27,28} (Figure 1A and 1B). The second patient was a 50-year old Chinese man who also had atrial fibrillation, complete atrioventricular block, ventricular tachyarrhythmia, and heart failure. Of his 4 siblings, 3 had similar cardiac conditions, and all had had an automatic implantable cardioverter defibrillator implanted. A heterozygous single-base exchange (1062C→T) in exon 6 of the *LMNA* gene resulting in a Q354X nonsense mutation was found to be cosegregated with the cardiac phenotype in this family

(Figure 1). The last patient was a 43-year-old Chinese man with atrial fibrillation, complete atrioventricular block, and ventricular tachyarrhythmia. A heterozygous single-base deletion (1554delC) at exon 9 of the *LMNA* gene was detected. According to our prediction of a second open reading frame with 1 “C” deletion at codon position 1554 in the *LMNA* mRNA transcript (NM_170707), the premature stop codon with sequence of “TGA” will be generated at an earlier position at the 547th amino acid, shortening the LMNA protein that is supposed to be transcribed (reduced from 665 to 547 amino acids) (Figure S1). This patient’s paternal uncle

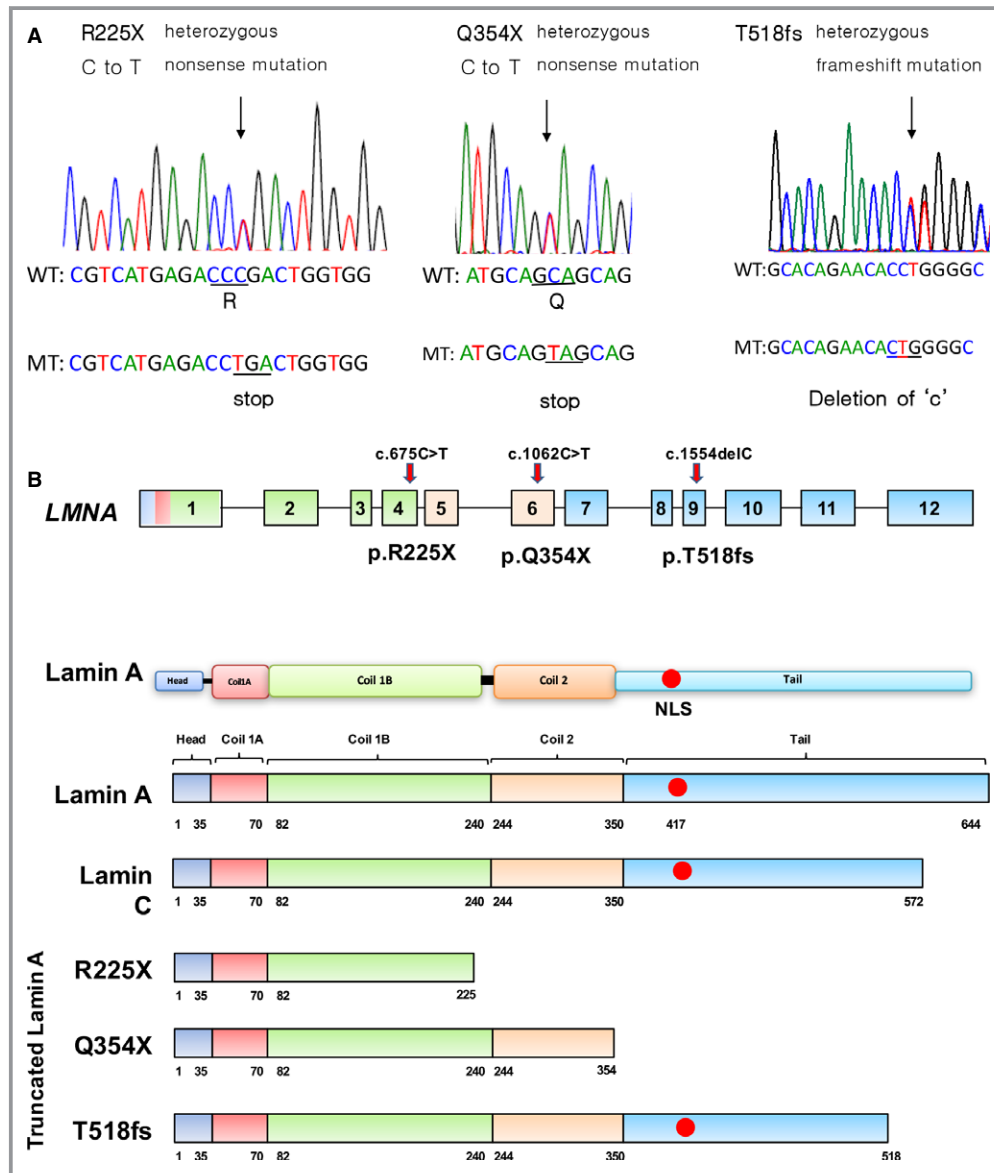


Figure 1. Schematic diagram illustrating the *LMNA* mutations involved in this study. A, Genetic disorders caused by nonsense and frame-shift mutations in *LMNA*. R225X yielded a premature stop codon, TGA, due to a C-to-T substitution; Q354X also yielded a premature stop codon, TAG, due to a C-to-T substitution; and the frameshift mutation T518fs resulted from a C deletion. B, Splice variant of *LMNA* gene yielding lamin A/C protein: the mutation yielded 3 different lengths of truncated lamin A/C protein. Key: NLS indicates nuclear localization signal.

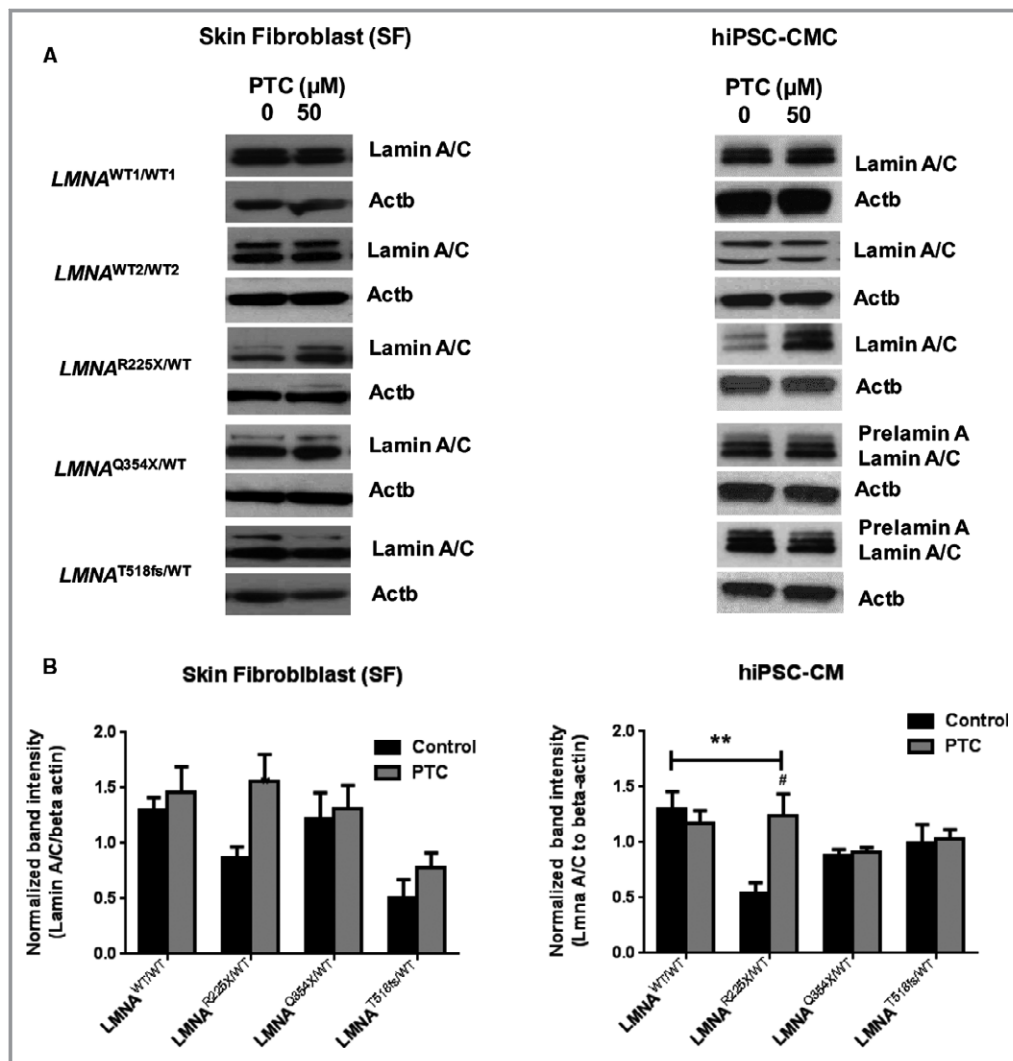


Figure 2. Effects of PTC124 on the expression of lamin A/C proteins in dermal fibroblasts and hiPSC-derived cardiomyocytes (hiPSC-CMC) derived from wild-type (*LMNA*^{WT1/WT1} and *LMNA*^{WT2/WT2}) and *LMNA* mutants (*LMNA*^{R225X/WT}, *LMNA*^{Q354X/WT}, and *LMNA*^{T518fs/WT}). A, Representative immunoblot and (B) quantitative data of protein-normalized lamin A/C protein expression. The band intensities of lamin A/C and β -actin (Actb) were measured from the high-resolution (300 \times 300 dots per inch) images using Image J. At least 3 to 6 independent samples were prepared for Western blot analysis. The significant difference of quantitative data was tested by 2-way ANOVA with post hoc Turkey multiple comparison test (** P <0.01 as indicated by arrows; # P <0.05, Control vs PTC). Original images of immunoblots in individual experiments are shown in Figure S2. hiPSC indicates human induced pluripotent stem cells.

had had atrial fibrillation and complete atrioventricular block (Figure 1A and 1B). Dermal fibroblasts were obtained from these patients during automatic implantable cardioverter defibrillator implantation, and patient-specific hiPSCs harboring the specific mutations were generated accordingly. The patient-specific *LMNA* mutations in these hiPSCs had been confirmed by genomic DNA sequencing analysis. For simplicity in description, the hiPSC lines containing the 672G \rightarrow T, 1062C \rightarrow T, and 1554delC mutations in 1 of the *LMNA* alleles will be denoted as R225X, Q354X, and T518fs mutants, respectively, in this article.

The commercially available hiPSC line (line IMR90, Wicell) and KS1 hiPSC line generated by our lab by lentiviral reprogramming that do not contain any *LMNA* mutations was used as a wild-type control in this study²¹ (Figure 1).

Effects of PTC124 on Expression of Lamin A/C Proteins in Dermal Fibroblasts and hiPSC-Derived Cardiomyocytes

First, we tested the effects of PTC124 on the level of lamin A/C proteins in dermal fibroblasts obtained from the 3 patients

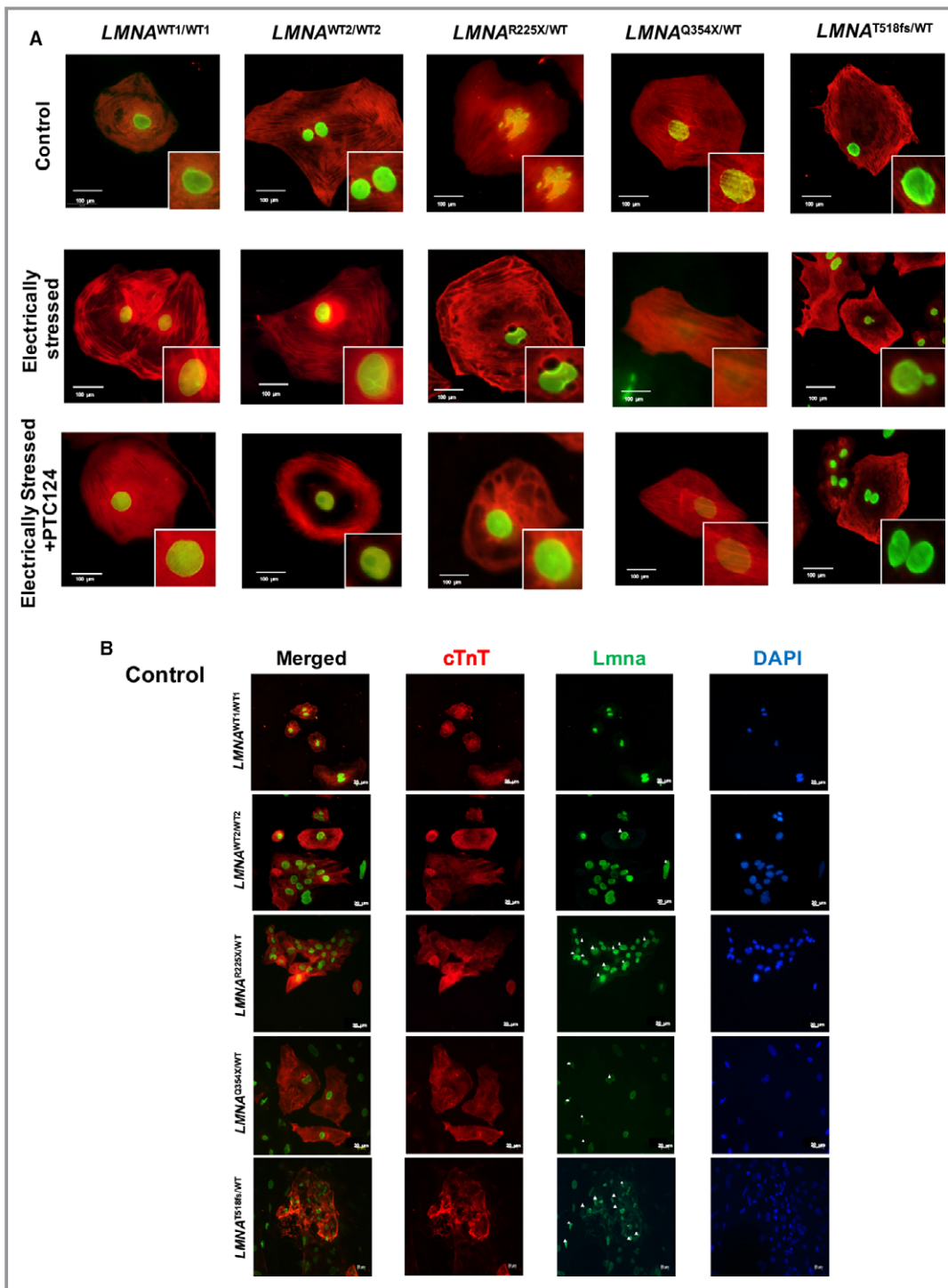


Figure 3. Nuclear blebbing in the hiPSC-derived cardiomyocytes. The 2 wild-type lines (*LMNA*^{WT1/WT1} and *LMNA*^{WT2/WT2}), R225X (*LMNA*^{R225X/WT}), Q354X (*LMNA*^{Q354/WT}), and T518fs (*LMNA*^{T518fs/WT}), mutant hiPSC lines were differentiated into cardiomyocytes and treated with PTC124. The occurrence of cardiac nuclear blebbing was revealed with coimmunostaining of cardiac troponin T (red) and lamin A/C (green). A, A single representative hiPSC CMC, and (B through D) representative images of lower magnification were used to quantify the portion of nuclear blebbing in a single field. At least 3 countings were performed. E, Quantitative data of nuclear blebbing count. The significant difference of quantitative data was tested by 2-way ANOVA with post hoc Turkey multiple comparison test (*****P*<0.0001 as indicated by arrows; ####*P*<0.0001 control vs treatment group). cTnT indicates cardiac troponin-T; DAPI, 4,6-diamidino-2-phenylindole dihydrochloride; hiPSC, human induced pluripotent stem cells; LMNA, lamin.

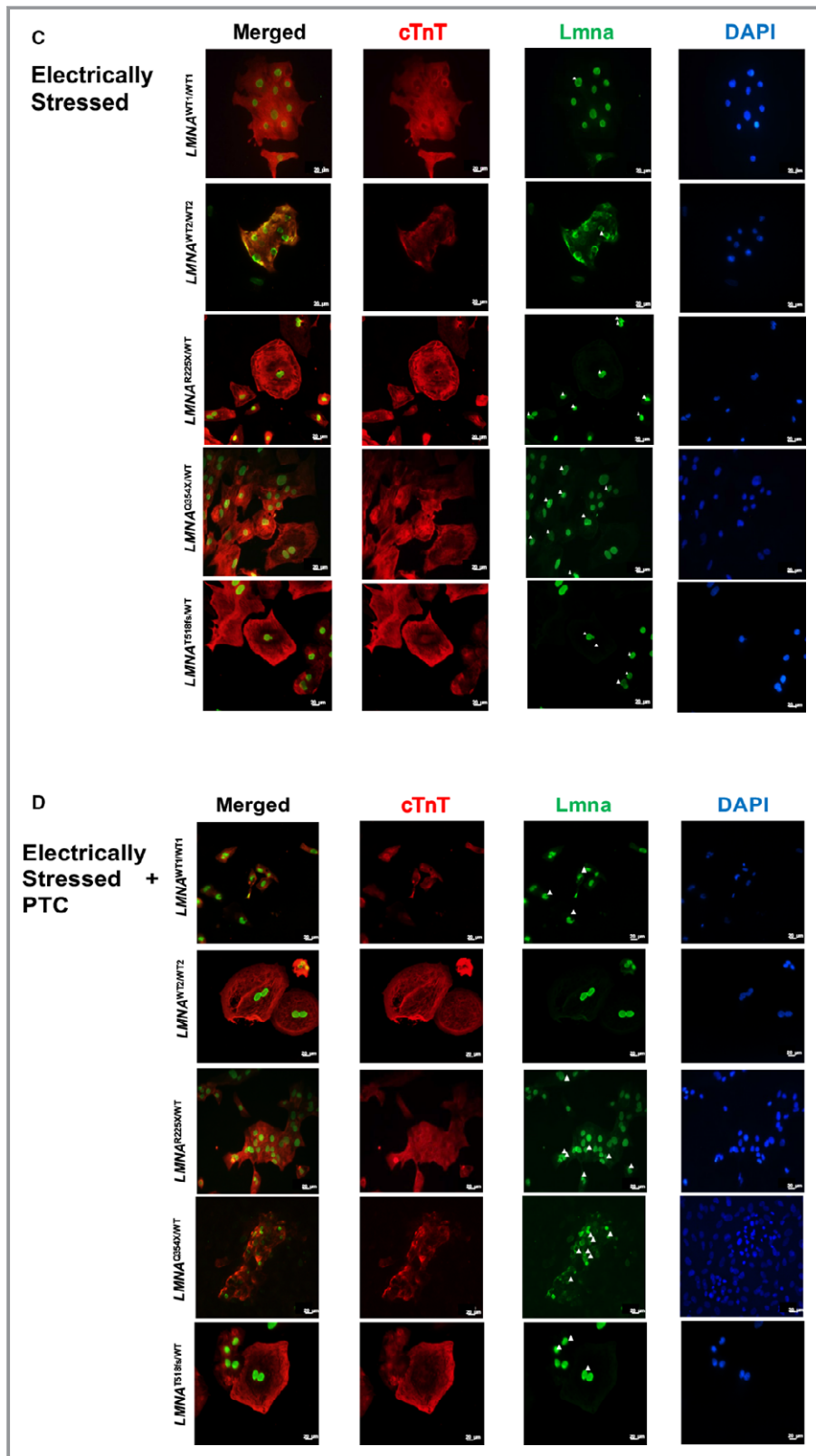


Figure 3. Continued

with *LMNA*-related cardiomyopathy (Figure 2). Dermal fibroblasts were treated with PTC124 (50 μmol/L), and the lamin A/C protein levels were evaluated by Western blotting

analysis. In the absence of PTC124, the translation yielded only intact lamin A/C products: a 74-kDa band indicating lamin A protein and a 63-kDa band from lamin C protein, in

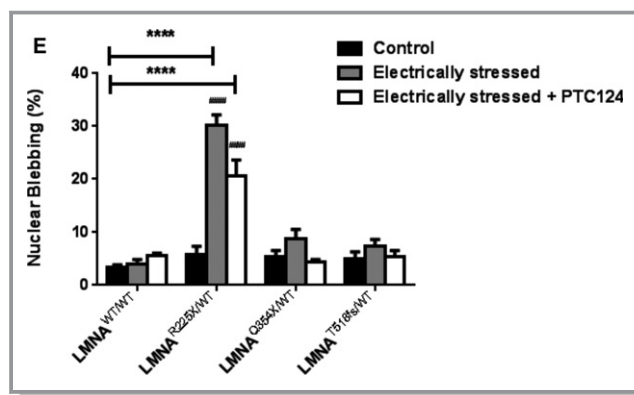


Figure 3. Continued

dermal fibroblasts from all 3 patients. No truncated lamin A/C protein was detected in any of the mutant lines (data not shown) (Figure 2). Compared with their wild-type counterpart, the levels of lamin A/C proteins were markedly reduced in dermal fibroblasts from all mutant lines. Treatment with PTC124 increased the level of both lamin A and C isoforms in dermal fibroblasts carrying the R225X mutation in the *LMNA* gene but not in the wild-type or dermal fibroblasts from the other 2 patients harboring Q354X or T518fs mutations. Importantly, as no prolonged lamin A/C protein products were detected, PTC124 treatment was not likely causing normal termination codon read-through.

Similar results were observed in the hiPSC-derived cardiomyocytes treated with PTC124. In brief, the level of lamin A/C proteins in all 3 mutant lines was substantially reduced compared with their wild-type counterpart in the absence of PTC124 (Figure 2). Similar to the findings observed in dermal fibroblasts, PTC124 treatment increased the level of both lamin A and C proteins in cardiomyocytes derived from the R225X mutant hiPSC line but not in those of the other 2 *LMNA* mutations (ie, Q354X and T518fs mutants). Interestingly, mild accumulation of prelamin A was observed in the cardiomyocytes derived from Q354X and T518fs mutants (Figure 2), regardless of the presence of PTC124 treatment.

Effects of PTC124 on Electrical Stimulation–Induced Nuclear Senescence and Apoptosis in hiPSC-Derived Cardiomyocytes

As previously reported by our team¹⁸ and others,²⁹ the nuclei of cardiomyocytes from *LMNA*-related cardiomyopathy often exhibit dysmorphic features such as micronucleation (blebbing), one of the hallmarks of nuclear senescence.³⁰ These changes together with apoptosis are often exaggerated in cardiomyocytes that are electrically active²⁹ or under constant electrical stress.¹⁸ As shown in Figure 3, coimmunostaining of lamin A/C (green) and cardiac troponin-T (red)

revealed that the cardiomyocytes derived from R225X or T518fs mutant lines exhibited nuclear blebbing even in the absence of external stress. After continuous electrical stressing, the nuclear blebbing events became more frequent in all the hiPSC-derived cardiomyocytes carrying *LMNA* mutations. Interestingly, the application of PTC124 alleviated nuclear senescent morphological abnormalities in the cardiomyocytes derived from the R225X mutant but not in those derived from the Q354X or T518fs mutant lines (Figure 3A through 3D). To evaluate the effects of PTC124 on apoptosis, we first performed TUNEL analysis. As shown in Figure 4A through 4D, in concordance with the nuclear blebbing assay, the electrical stress-induced apoptosis in cardiomyocytes with R225X mutation was markedly reduced in the presence of PTC124 (Figure 4B). Nonetheless, no significant changes in apoptosis were detected on application of PTC124 in the other 2 mutants (Figure 4C through 4D). In order to provide more quantitative assessment of the protective effects of PTC124 against electrical stress-induced apoptosis, we further quantified the proportion of apoptotic cells using the APO-BrdU TUNEL assay (Figure 4F through 4G and Table S1). Compared with the wild-type control, all 3 mutants showed a significantly higher proportion of apoptotic cardiomyocytes. On electrical stressing, the proportion of apoptotic cells increased markedly by 40.58% ($n=3-7$, $P<0.05$) only in hiPSC-derived cardiomyocytes with the R225X mutation (Figure 4G). More importantly, application of PTC124 significantly reduced the electrical stimulation-induced apoptotic population by 41.89% in cardiomyocytes derived from R225X mutant ($n=3-5$; $P<0.05$). Neither electrical stress nor the application of PTC124 caused any statistically significant changes to the proportion of apoptotic cells in any of the other groups.

Nonsense *LMNA* mRNA Degradation

In addition to defective translation as a result of the nonsense mutations, the suppressed production of lamin

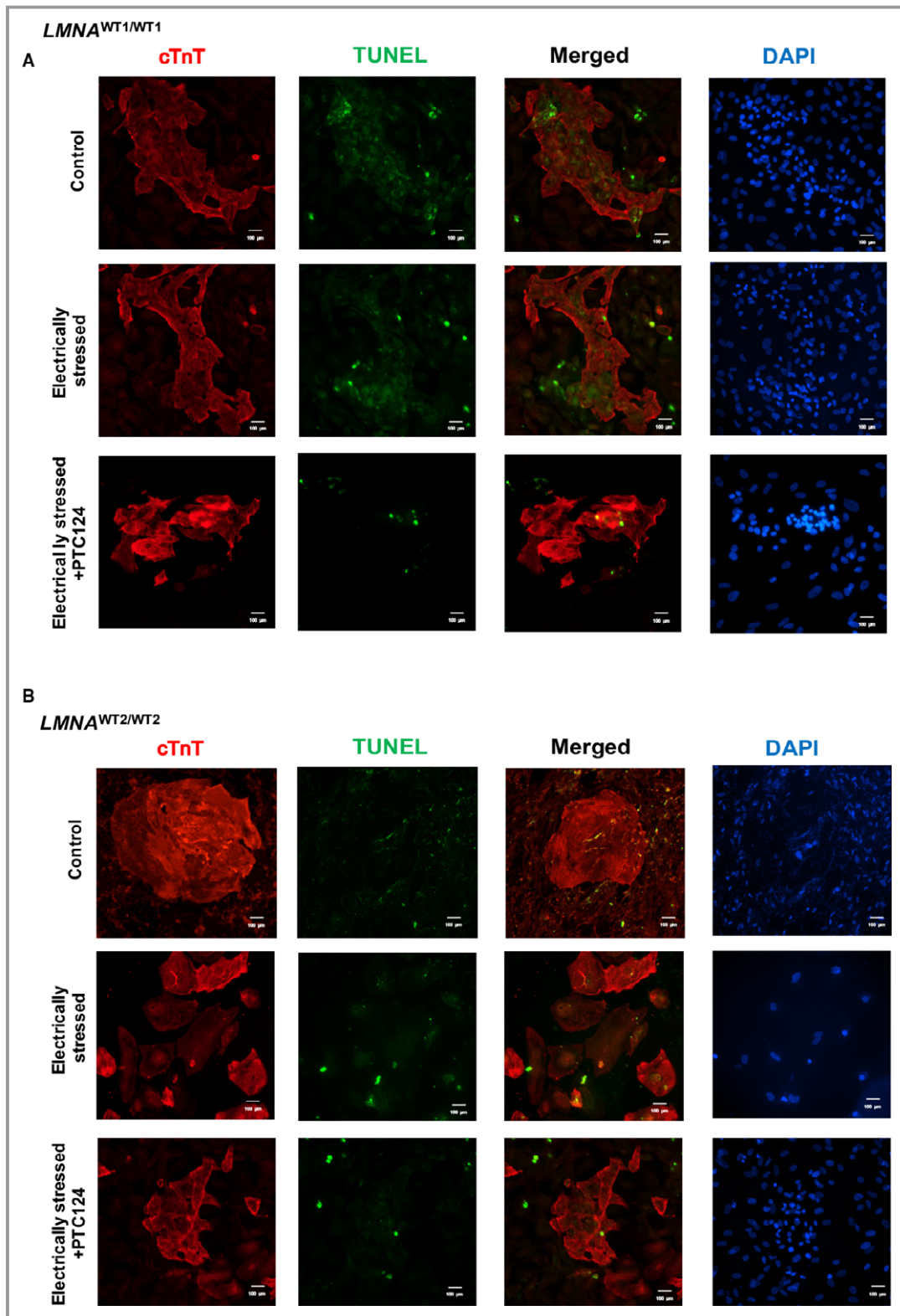


Figure 4. Evaluation of TUNEL-positive apoptotic cell in electrically stressed and PTC124-treated cardiomyocytes derived from wild-type (*LMNA*^{WT1/WT1} and *LMNA*^{WT2/WT2}) and *LMNA* mutants (*LMNA*^{R225X/WT}, *LMNA*^{O354X/WT}, and *LMNA*^{T518fs/WT}) by (A through E) immunostaining; (F through G) and also by Apo-BrdU TUNEL-FACS analysis to quantify apoptotic cells (Significant difference was analyzed by 2-way ANOVA with Tukey multiple comparison post-hoc test **P*<0.05; *n*=3 to 5 (as indicted by arrows) and (control vs electrically stressed) #*P*<0.05; *n*=3 to 7). FACS indicates fluorescence-activated cell sorting; TUNEL, terminal deoxynucleotidyl transferase dUTP nick end labeling.

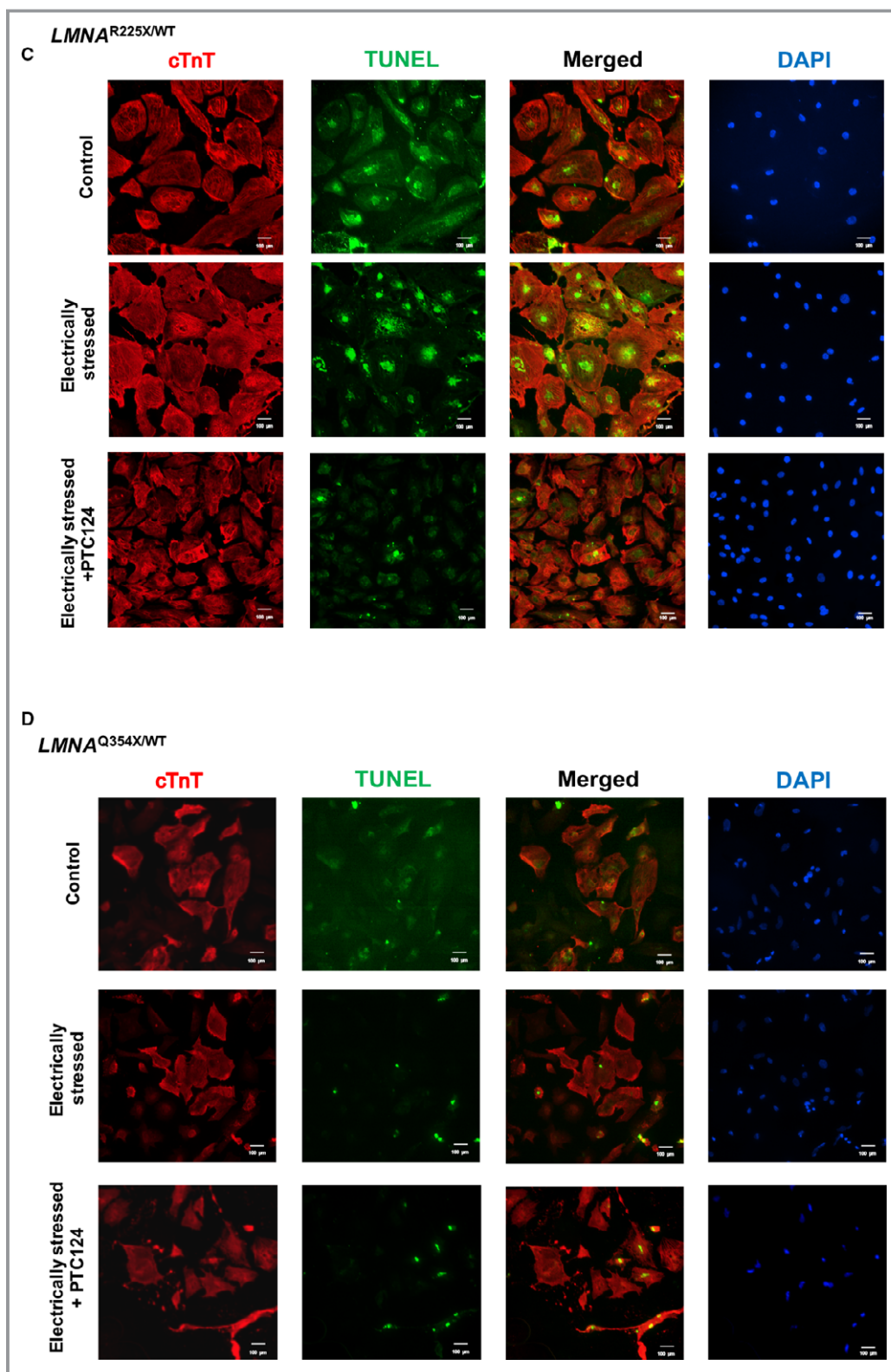


Figure 4. Continued

A/C proteins could be due to a nonsense-mediated mRNA decay mechanism.³¹ To evaluate such a possibility, we precisely quantified the *LMNA* mRNA level in cardiomyocytes

derived from the wild-type and mutant lines using *Taqman* real-time polymerase chain reaction assay. As shown in Figure 5, the relative cardiac *LMNA* expression in all 3

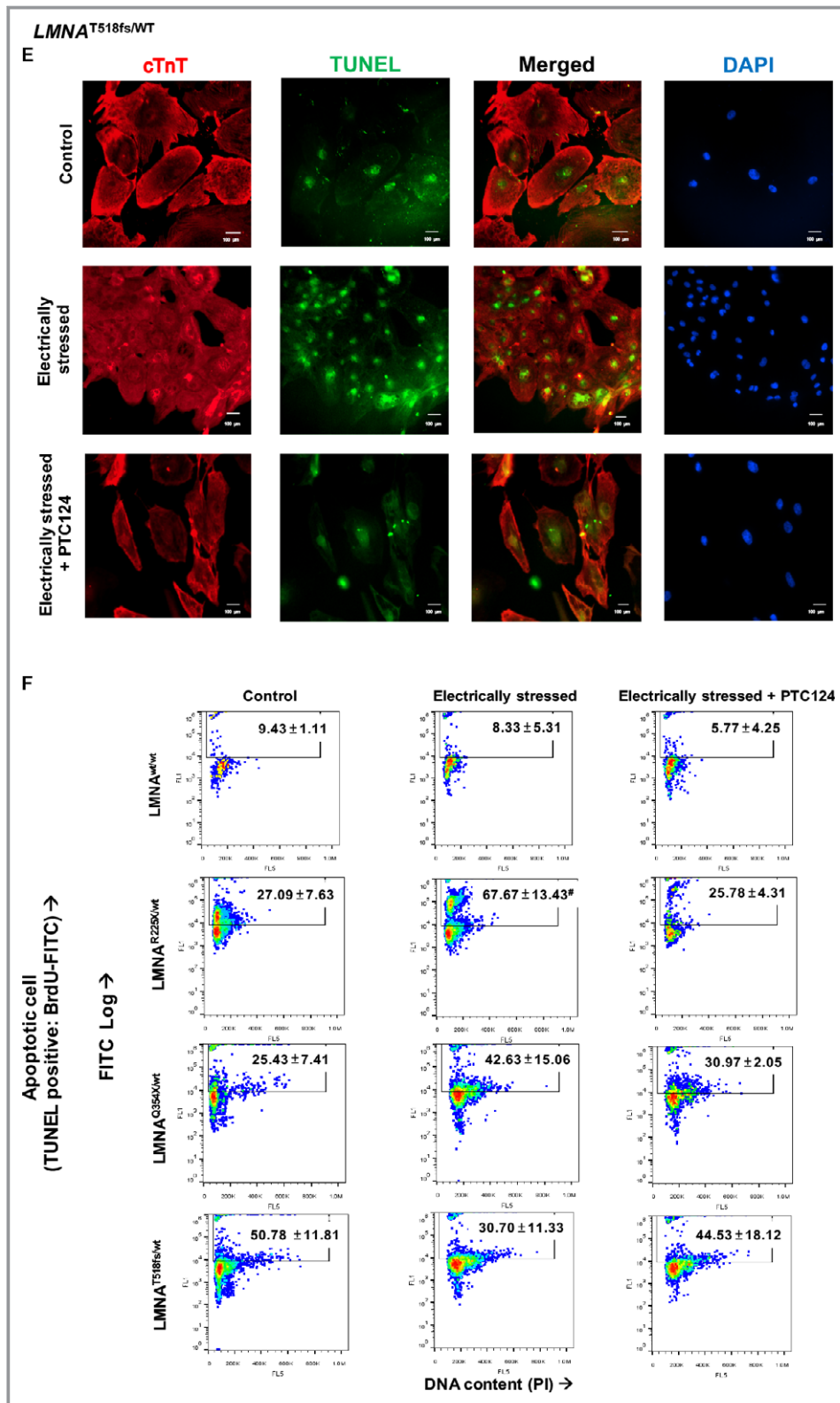


Figure 4. Continued

mutants was significantly lower than that in the wild-type control. This suggests that nonsense mRNA degradation may contribute to the reduced lamin A/C protein level.

Interestingly, PTC124 could not restore the mRNA production in any mutant line, suggesting that its activity was limited to a translational level.

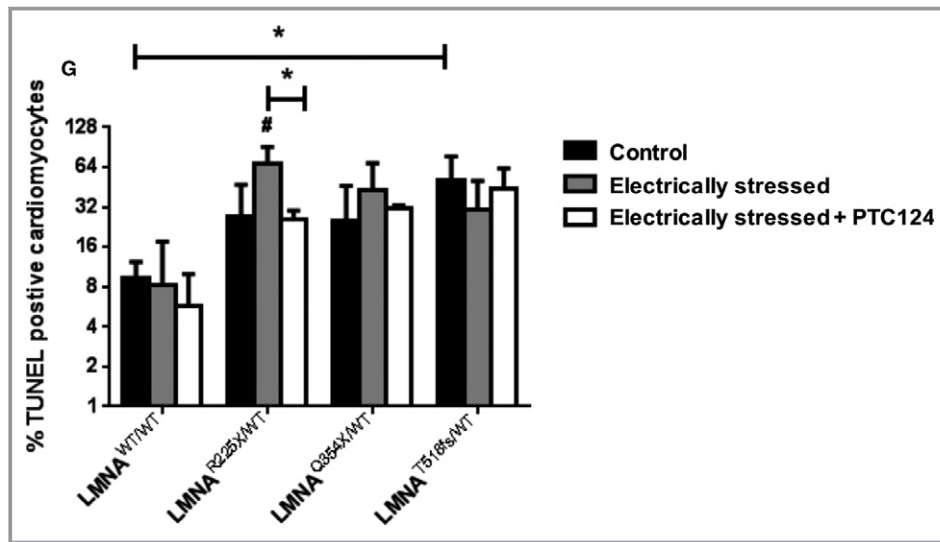


Figure 4. Continued

Effects of PTC124 on Excitation-Contraction Coupling in Cardiomyocytes Derived From the R225X Mutant hiPSC

Because the PTC124-mediated reduction in apoptosis was observed only in the cardiomyocytes derived from the R225X mutant and not in other lines, we further evaluated the effects of PTC124 on excitation-contraction coupling, calcium homeostasis, and contractile abnormalities in this particular line. Contractilities and calcium transients were recorded

simultaneously under field electrical pacing at frequencies ranging from 0.5 Hz to 2 Hz. As shown in Figure 6A, hiPSC-derived cardiomyocytes (both wild-type and mutants) were responsive to electrical pacing and showed comparable diastolic and peak calcium levels (Figure 6B and 6D). Diastolic calcium levels (indicated by the baseline levels of the calcium transient tracings) of both lines increased as the pacing frequency increased (Figure 6B). In general, the maximum calcium released (indicated by the peak amplitude of the calcium transient tracings) in cardiomyocytes derived from the R225X mutant was less than that released in the wild-type counterparts (Figure 6C). The systolic cell length also reduced remarkably in the mutant cardiomyocytes treated with PTC124, indicating a more efficient coupling between intracellular calcium surge and cellular contraction (Figure 6E). Regardless of the application of PTC124, there was no significant change in the upstroke velocity (ie, the rate of calcium release) of calcium transients or rate of cell shortening between wild-type and mutant hiPSC-derived cardiomyocytes (Figure 6F and 6G). Nevertheless, at high pacing speed (2 Hz), PTC124 significantly improved the rate of calcium reuptake in the mutant cardiomyocytes (as indicated by a more negative value of V_{max} decay) ($P < 0.05$, $n = 3$) (Figure 6H). Furthermore, PTC124 treatment appeared to improve the rate of cellular relengthening in the mutant cardiomyocytes (Figure 6I).

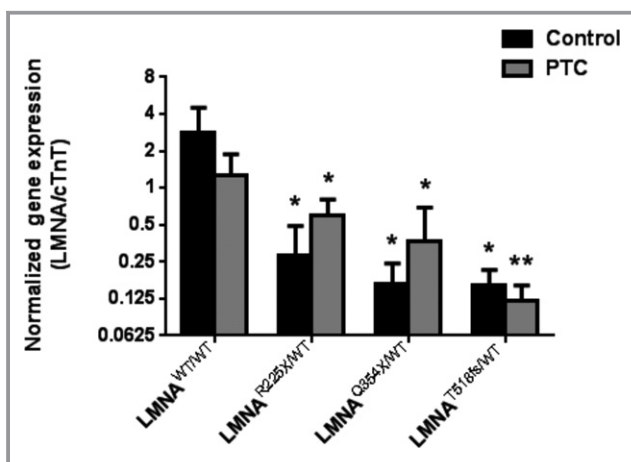


Figure 5. Normalized gene expression level of *LMNA* in PTC124-treated hiPSC-derived cardiomyocytes. The endogenous control gene was *TUBB*, and *TNNT2* was used to normalize the number of cardiac cells within the differentiated population. Significant difference was analyzed by 1-way ANOVA with Tukey multiple comparison post hoc test compared with wild-type control group, $*P < 0.05$ and $**P < 0.01$; $n = 5$. hiPSC indicates human induced pluripotent stem cells.

Discussion

Precision medicine, according to the National Institutes of Health in the United States, is an emerging approach for disease treatment and prevention that takes into account

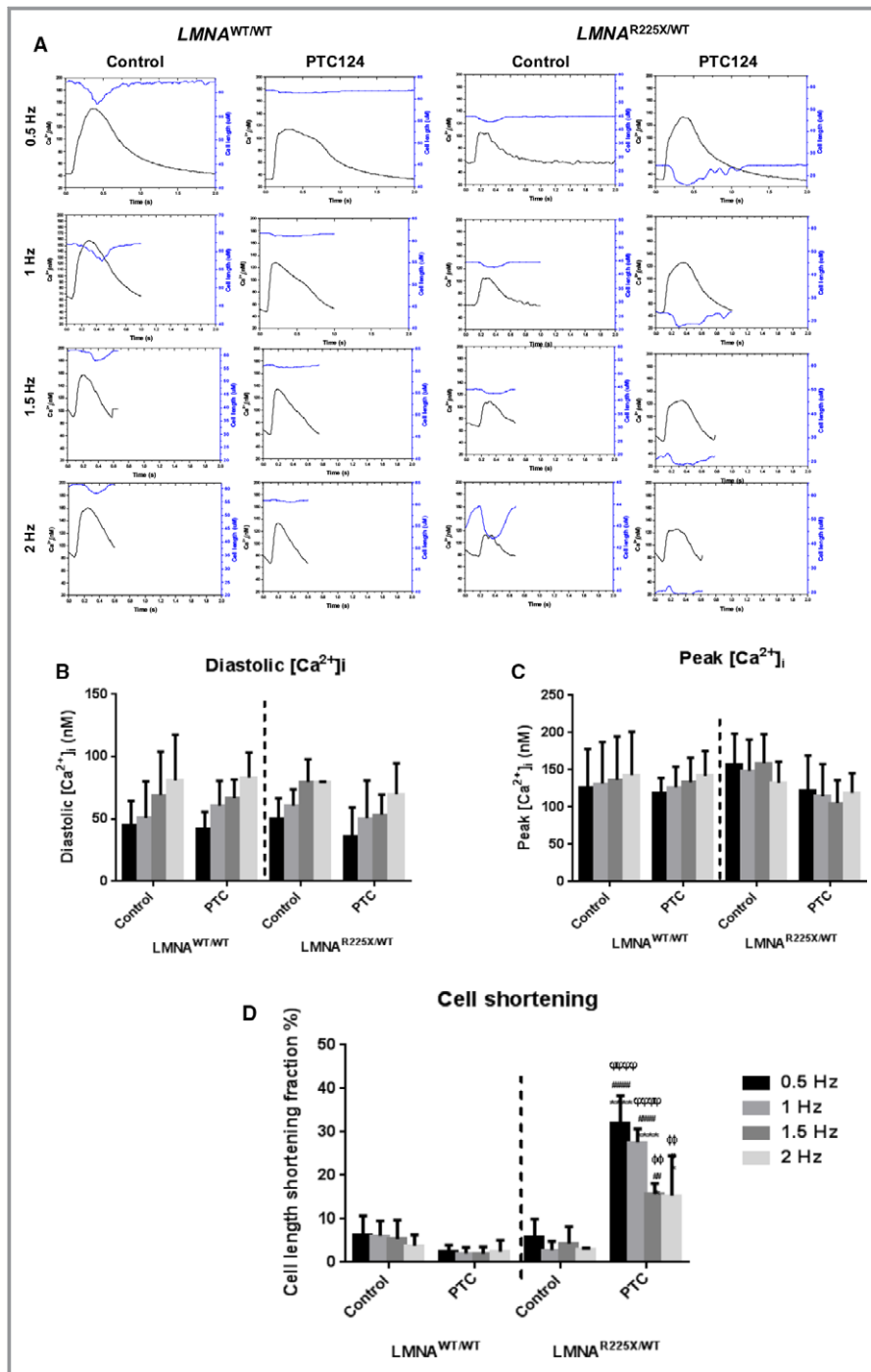


Figure 6. Excitation-contraction (EC) coupling was improved by PTC124 in the cardiomyocytes derived from the R255X mutant. A, Representative tracing of calcium transient and cell-shortening in *LMNA*^{WT/WT} and *LMNA*^{R225X/WT} cells treated with PTC124. Rate dependence of calcium transients and cell contractility pacing frequency range of 0.5, 1, and 1.5 to 2 Hz are shown in terms of (B) diastolic calcium, (C) peak calcium amplitude, (D) fractional shortening (%) (**P*<0.05; n=5 to 7; WT: PTC vs R225X:PTC #####*P*<0.0001; R225X: 0.5-Hz control vs R225X: 0.5-Hz or 1-Hz PTC: φ φ φ φ *P*<0.0001; R225X: 0.5 Hz PTC vs R225X: 1.5 or 2 Hz PTC: φ φ *P*<0.001); (E and F) maximal upstroke velocity (*V*_{max} upstroke) of calcium transient and rate of cell shortening (ie, contraction); (G and H) maximal decay velocity (*V*_{max} decay) and rate of cell relengthening (ie relaxation). Improved calcium decay kinetics and relaxation performance are shown (G and H). Significant difference was analyzed by comparing pacing rate of 0.5 Hz with the other rates of the same treatment group in 1 cell line, or otherwise indicated by arrows using 2-way ANOVA with Turkey test as post hoc (**P*<0.05).

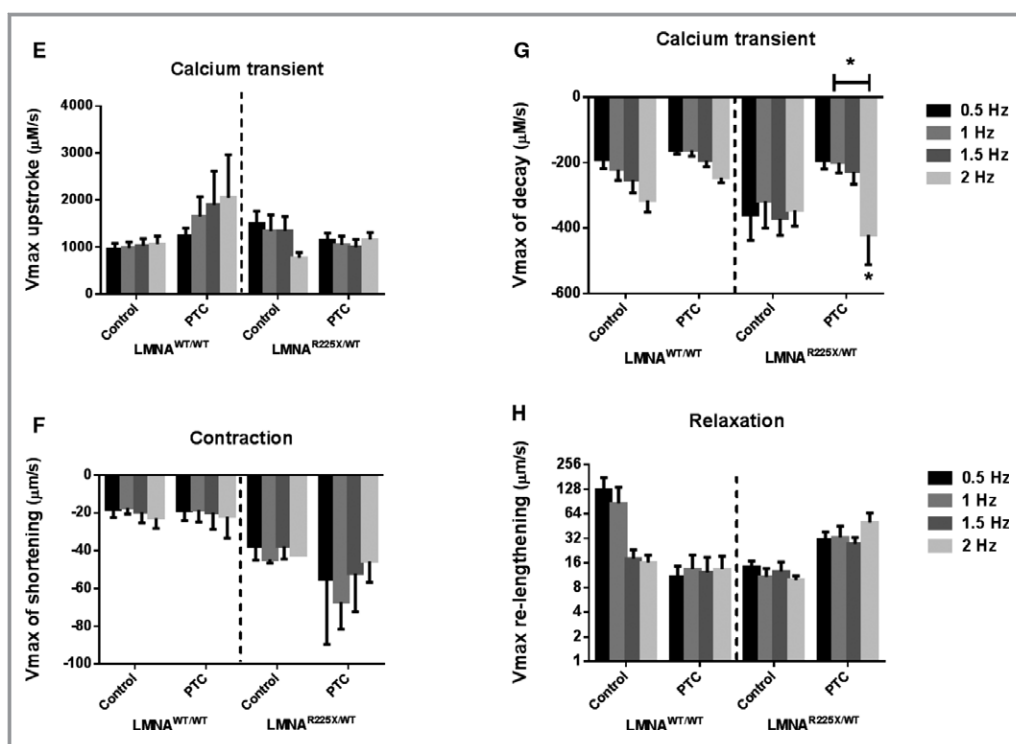


Figure 6. Continued

individual variability in environment, lifestyle, and genetic makeup for individual patients.^{32,33} The assumption is that differences in an individual patient's genetic makeup as well as environmental factors contribute to his or her differential clinical outcome, particularly in responsiveness to treatments. In other words, patients with apparently similar clinical conditions may be treated differently because of these individual differences. Over the past 3 decades, there has been tremendous progress in genetics research that has identified numerous genes responsible for dilated cardiomyopathies and provided novel insight into their pathogenic mechanisms. Nonetheless, translation of these research findings to clinical practice remains incomplete. In fact, even with the availability of an individual patient's genetic information that underlies dilated cardiomyopathies, a disease-specific intervention designed to tackle the root causes of the condition is rarely available. As a result, despite different genetic etiologies and pathogeneses, dilated cardiomyopathies are often treated similarly simply based on clinical presentations.

Mutations in *LMNA* genes are the most common cause of familial dilated cardiomyopathy, particularly among those with concomitant atrioventricular conduction block.^{7,8} In our study, despite different mutations in the 3 patients with *LMNA*-related cardiomyopathy, their clinical presentations were remarkably similar with early onset atrioventricular block and atrial fibrillation around the fourth decade of life, followed by ventricular tachyarrhythmia and heart failure in the fifth to

sixth decade of life. The condition was inherited in an autosomal dominant pattern in all 3 families. In accordance with their genotypes, both dermal fibroblasts and cardiomyocytes derived from R225X, Q354X, and T518fs mutants displayed reduced lamin A/C protein production. As demonstrated in our previous hiPSC-based model of *LMNA*-related cardiomyopathy,¹⁸ cardiomyocytes derived from these 3 mutants exhibited nuclear senescence and apoptosis that were aggravated in the presence of electrical stress. Nonetheless, despite their very similar clinical presentations and cellular phenotypes, there was a differential effect of PTC124 on lamin A/C protein production in their primary dermal fibroblasts (R225X>>Q354X and T518fs). Similar to dermal fibroblasts, PTC124 restored lamin A/C protein production only in cardiomyocytes derived from the R225X mutants but not in their Q354X or T518fs counterparts. More importantly, the increase in lamin A/C production was associated with alleviated nuclear senescence and reduced apoptosis. Furthermore, PTC124 treatment improved the excitation-contraction coupling and contractile functions of the hiPSC-derived cardiomyocytes carrying the R225X mutation.

The lack of responsiveness to PTC124 of cardiomyocytes derived from the T518fs mutant, which served as a negative control, is expected. On the contrary, for the cardiomyocytes derived from the Q354X mutant, the lack of efficiency could be explained by the difference in nucleotide sequence of the mutant premature stop codons. Nonsense mutations are

point mutations that result in the occurrence of 1 of 3 stop codons, UAG, UAA, or UGA, in the messenger RNA coding region, leading to a truncated protein product due to premature termination of mRNA translation and/or promotion of mRNA destabilization by nonsense-mediated mRNA decay. Although PTC124 promotes read-through of all 3 nonsense codons, its potency differs according to the nucleotide sequences of the premature stop codons, with the highest read-through at UGA, followed by UAG, and then UAA.¹⁰ For the 2 nonsense mutations, the R225X mutation in the *LMNA* gene is a result of a premature stop codon (UGA) that is the most PTC124-responsive nucleotide sequence, whereas in the Q354X mutant, the sequence of the stop codon is UAG, which seems to be less PTC124 responsive. Because the efficacy of the translational read-through of premature stop codons and production of full-length proteins by interfering with ribosomal proofreading depend on the availability of nonsense transcripts to the ribosomal translational machinery, it is interesting that in our study, application of PTC124 increased mRNA expression of the 2 nonsense transcripts: R225X and Q354X. Nonetheless, it is beyond the scope of the present study to determine whether PTC124 can affect the efficiency of the nonsense mutation mRNA decay mechanisms.

For nonsense mutation, it seems to be stating the obvious that translational read-through of premature stop codons with PTC124 is expected to produce full-length proteins and reverse the pathogenic process. Nonetheless, in a recent study using hiPSC-derived cardiomyocytes from 2 patients who harbored nonsense mutations in the sodium channel gene *SCN5A*, R1638X and W156X, although the premature stop codon sequences in both mutations were the most optimum sequence for PTC124, UGA, PTC124 and gentamicin, another premature stop codon read-through agent, failed to restore sodium current I_{Na} .³⁴ Although the sodium channel protein level was not quantified to document the restored protein translation, other downstream mechanisms such as a trafficking defect might have been responsible. This reinforces the need for precision medicine. hiPSC technology and in vitro drug testing strategies provide unparalleled opportunities to realize the promise of precision medicine. This strategy may be exploited to select the patients with maximum drug responsiveness for standard clinical trials. Then, the expected drug effects may be much larger, and the required sample size would then be much smaller, making standard randomized clinical trials possible.

Conclusions

Taken collectively, PTC124 promoted translation read-through of premature stop codons in patient-specific hiPSC-derived cardiomyocytes that harbored the mutation R225X in the

LMNA gene and alleviated nuclear senescence, apoptosis, and altered excitation-contraction coupling. The same effects were not evident in patient-specific hiPSC-derived cardiomyocytes that harbored another nonsense mutation or a frame-shift mutation. Based on our data, hiPSC technology represents a general approach to predict the clinical response of patients with an apparently similar clinical condition and to realize the potential of precision medicine.

Acknowledgments

We are thankful for the technical support provided by Dr Au.

Disclosures

None.

References

- Lin F, Worman HJ. Structural organization of the human gene encoding nuclear lamin A and nuclear lamin C. *J Biol Chem*. 1993;268:16321–16326.
- Capell BC, Collins FS. Human laminopathies: nuclei gone genetically awry. *Nat Rev*. 2006;7:940–952.
- Burke B, Stewart CL. The laminopathies: the functional architecture of the nucleus and its contribution to disease. *Annu Rev Genomics Hum Genet*. 2006;7:369–405.
- Dreesen O, Stewart CL. Accelerated aging syndromes, are they relevant to normal human aging? *Aging*. 2011;3:889–895.
- Rankin J, Ellard S. The laminopathies: a clinical review. *Clin Genet*. 2006;70:261–274.
- Worman HJ, Fong LG, Muchir A, Young SG. Laminopathies and the long strange trip from basic cell biology to therapy. *J Clin Invest*. 2009;119:1825–1836.
- Fatkin D, Otway R, Richmond Z. Genetics of dilated cardiomyopathy. *Heart Fail Clin*. 2010;6:129–140.
- Dellefave L, McNally EM. The genetics of dilated cardiomyopathy. *Curr Opin Cardiol*. 2010;25:198–204.
- Wolf CM, Wang L, Alcalai R, Pizard A, Burgon PG, Ahmad F, Sherwood M, Branco DM, Wakimoto H, Fishman GI, See V, Stewart CL, Conner DA, Berul CI, Seidman CE, Seidman JG. Lamin a/c haploinsufficiency causes dilated cardiomyopathy and apoptosis-triggered cardiac conduction system disease. *J of mol and cell cardiol*. 2008;44:293–303.
- Welch EM, Barton ER, Zhuo J, Tomizawa Y, Friesen WJ, Trifillis P, Paushkin S, Patel M, Trotta CR, Hwang S, Wilde RG, Karp G, Takasugi J, Chen G, Jones S, Ren H, Moon YC, Corson D, Turpoff AA, Campbell JA, Conn MM, Khan A, Almstead NG, Hedrick J, Mollin A, Risher N, Weetall M, Yeh S, Branstrom AA, Colacino JM, Babiak J, Ju WD, Hirawat S, Northcutt VJ, Miller LL, Spatrick P, He F, Kawana M, Feng H, Jacobson A, Peltz SW, Sweeney HL. Ptc124 targets genetic disorders caused by nonsense mutations. *Nature*. 2007;447:87–91.
- Du M, Liu X, Welch EM, Hirawat S, Peltz SW, Bedwell DM. Ptc124 is an orally bioavailable compound that promotes suppression of the human CFTR-G542X nonsense allele in a CF mouse model. *Proc Natl Acad Sci USA*. 2008;105:2064–2069.
- Hirawat S, Welch EM, Elfring GL, Northcutt VJ, Paushkin S, Hwang S, Leonard EM, Almstead NG, Ju W, Peltz SW, Miller LL. Safety, tolerability, and pharmacokinetics of PTC124, a nonaminoglycoside nonsense mutation suppressor, following single- and multiple-dose administration to healthy male and female adult volunteers. *J Clin Pharmacol*. 2007;47:430–444.
- Clinicaltrials.gov. A phase 3 efficacy and safety study of ataluren (PTC124[®]) in patients with nonsense mutation cystic fibrosis. <https://clinicaltrials.gov/ct2/show/study/NCT02139306>. Accessed January 1, 2017.
- Tse HF, Ho JC, Choi SW, Lee YK, Butler AW, Ng KM, Siu CW, Simpson MA, Lai WH, Chan YC, Au KW, Zhang J, Lay KW, Esteban MA, Nicholls JM, Colman A, Sham PC. Patient-specific induced-pluripotent stem cells-derived cardiomyocytes recapitulate the pathogenic phenotypes of dilated cardiomyopathy due to a novel DES mutation identified by whole exome sequencing. *Hum Mol Genet*. 2013;22:1395–1403.

15. Ng KM, Mok PY, Butler AW, Ho JC, Choi SW, Lee YK, Lai WH, Au KW, Lau YM, Wong LY, Esteban MA, Siu CW, Sham PC, Colman A, Tse HF. Amelioration of X-linked related autophagy failure in Danon disease with DNA methylation inhibitor. *Circulation*. 2016;134:1373–1389.
16. Lee YK, Lau YM, Ng KM, Lai WH, Ho SL, Tse HF, Siu CW, Ho PW. Efficient attenuation of Friedreich's ataxia (FRDA) cardiomyopathy by modulation of iron homeostasis—human induced pluripotent stem cell (hiPSC) as a drug screening platform for FRDA. *Int J Cardiol*. 2016;203:964–971.
17. Ho JC, Zhou T, Lai WH, Huang Y, Chan YC, Li X, Wong NL, Li Y, Au KW, Guo D, Xu J, Siu CW, Pei D, Tse HF, Esteban MA. Generation of induced pluripotent stem cell lines from 3 distinct laminopathies bearing heterogeneous mutations in lamin A/C. *Aging*. 2011;3:380–390.
18. Siu CW, Lee YK, Ho JC, Lai WH, Chan YC, Ng KM, Wong LY, Au KW, Lau YM, Zhang J, Lay KW, Colman A, Tse HF. Modeling of lamin A/C mutation premature cardiac aging using patient-specific induced pluripotent stem cells. *Aging*. 2012;4:803–822.
19. Lee YK, Ho PW, Schick R, Lau YM, Lai WH, Zhou T, Li Y, Ng KM, Ho SL, Esteban MA, Binah O, Tse HF, Siu CW. Modeling of Friedreich ataxia-related iron overloading cardiomyopathy using patient-specific-induced pluripotent stem cells. *Pflugers Arch*. 2014;466:1831–1844.
20. Sayed N, Liu C, Wu JC. Translation of human-induced pluripotent stem cells: from clinical trial in a dish to precision medicine. *J Am Coll Cardiol*. 2016;67:2161–2176.
21. Lai WH, Ho JC, Lee YK, Ng KM, Au KW, Chan YC, Lau CP, Tse HF, Siu CW. Rock inhibition facilitates the generation of human-induced pluripotent stem cells in a defined, feeder-, and serum-free system. *Cell Reprogram*. 2010;12:641–653.
22. Lian X, Zhang J, Azarin SM, Zhu K, Hazeltine LB, Bao X, Hsiao C, Kamp TJ, Palecek SP. Directed cardiomyocyte differentiation from human pluripotent stem cells by modulating Wnt/ β -catenin signaling under fully defined conditions. *Nat Protoc*. 2013;8:162–175.
23. Kuramochi Y, Guo X, Sawyer DB, Lim CC. Rapid electrical stimulation induces early activation of kinase signal transduction pathways and apoptosis in adult rat ventricular myocytes. *Exp Physiol*. 2006;91:773–780.
24. Ho JC, Lai WH, Li MF, Au KW, Yip MC, Wong NL, Ng ES, Lam FF, Siu CW, Tse HF. Reversal of endothelial progenitor cell dysfunction in patients with type 2 diabetes using a conditioned medium of human embryonic stem cell-derived endothelial cells. *Diabetes Metab Res Rev*. 2012;28:462–473.
25. Chan YC, Ting S, Lee YK, Ng KM, Zhang J, Chen Z, Siu CW, Oh SK, Tse HF. Electrical stimulation promotes maturation of cardiomyocytes derived from human embryonic stem cells. *J Cardiovasc Transl Res*. 2013;6:989–999.
26. Ng KM, Lee YK, Lai WH, Chan YC, Fung ML, Tse HF, Siu CW. Exogenous expression of human apoA-I enhances cardiac differentiation of pluripotent stem cells. *PLoS One*. 2011;6:e19787.
27. Saga A, Karibe A, Otomo J, Iwabuchi K, Takahashi T, Kanno H, Kikuchi J, Keitoku M, Shinozaki T, Shimokawa H. Lamin A/C gene mutations in familial cardiomyopathy with advanced atrioventricular block and arrhythmia. *Tohoku J Exp Med*. 2009;218:309–316.
28. van Tintelen JP, Hofstra RM, Katerberg H, Rossenbacker T, Wiesfeld AC, du Marchie Sarvaas GJ, Wilde AA, van Langen IM, Nannenber EA, van der Kooij AJ, Kraak M, van Gelder IC, van Veldhuisen DJ, Vos Y, van den Berg MP; Working Group on Inherited Cardiac Disorders, line 27/50, Interuniversity Cardiology Institute of The Netherlands. High yield of LMNA mutations in patients with dilated cardiomyopathy and/or conduction disease referred to cardiogenetics outpatient clinics. *Am Heart J*. 2007;154:1130–1139.
29. Nikolova V, Leimena C, McMahon AC, Tan JC, Chandar S, Jogia D, Kesteven SH, Michalick J, Otway R, Verheyen F, Rainer S, Stewart CL, Martin D, Feneley MP, Fatkin D. Defects in nuclear structure and function promote dilated cardiomyopathy in lamin A/C-deficient mice. *J Clin Invest*. 2004;113:357–369.
30. Righolt CH, van't Hoff ML, Vermolen BJ, Young IT, Raz V. Robust nuclear lamina-based cell classification of aging and senescent cells. *Aging*. 2011;3:1192–1201.
31. Mendell JT, Dietz HC. When the message goes awry: disease-producing mutations that influence mRNA content and performance. *Cell*. 2001;107:411–414.
32. National Institutes of Health. Precision medicine initiative cohort program. <https://www.nih.gov/epoxy1.lib.hku.hk/precision-medicine-initiative-cohort-program>. Accessed January 13, 2016.
33. Collins FS, Varmus H. A new initiative on precision medicine. *N Engl J Med*. 2015;372:793–795.
34. Kosmidis G, Veerman CC, Casini S, Verkerk AO, van de Pas S, Bellin M, Wilde AA, Mummery CL, Bezzina CR. Readthrough-promoting drugs gentamicin and PTC124 fail to rescue Nav1.5 function of human-induced pluripotent stem cell-derived cardiomyocytes carrying nonsense mutations in the sodium channel gene *SCN5A*. *Circ Arrhythm Electrophysiol*. 2016;9:e004227.

SUPPLEMENTAL MATERIAL

Table S1. Raw data of apoptotic assay of the effects of PTC124 on electrically-stressed hiPSC-CMs by Apo-BrdU-TUNEL FACS analysis

Cell line	Treatment group	Number of cell		% of Apoptotic cell
		Total	Apoptotic (TUNEL-positive)	
LMNA ^{WT/WT}	Control	1655	136	8.20
		1604	113	7.00
		1181	134	11.30
		650	72	11.10
		1505	211	14.00
		1546	140	9.10
	Electrically stressed	2457	129	5.30
		693	129	18.80
		8679	132	1.50
	Electrically stressed + PTC124	1265	60	4.70
		776	10	14.20
		1360	10	0.70
8640		210	2.40	
LMNA ^{R225X/WT}	Control	1587	132	8.30
		4923	1653	38.50
		260	132	50.80
		2736	291	10.60
		3973	343	8.60
		692	131	18.90
		1532	826	53.90
	Electrically stressed	3642	1547	42.50
		272	196	72.10
		2062	1822	88.40
	Electrically stressed + PTC124	272	196	37.10
		2293	415	18.10
		8282	1572	19.00
		875	168	19.20
		152	54	35.50
LMNA ^{Q354X/WT}	Control	689	75	10.90
		953	108	11.30
		395	54	13.70
		278	198	71.20
		2003	565	28.90
		1909	311	16.30
		593	75	12.60
	Electrically stressed	1385	533	38.50
		149	110	73.80
		2780	625	22.50
	Electrically stressed + PTC124	1052	350	33.30
		900	314	34.90
1615		453	28.00	
2500		750	30.00	
LMNA ^{T518fs/WT}	Control	128	97	75.80
		220	124	56.40
		2266	1708	75.40
		1474	332	22.50
		1200	286	23.80
	Electrically stressed	608	321	52.80
		3549	543	15.30
		1426	342	24.00
	Electrically stressed + PTC124	261	207	79.30
		2255	413	18.30
1152		415	36.00	

Figure S1.

A Translation of *LMNA* wild type transcript (NM_170707)

1	atg	gag	acc	cgg	tcc	gag	acc	cgg	cgc	gcc	acc	cgc	agc	ggg	gcg	cag	45	811	ctg	gac	aat	gcc	agg	cag	tct	gct	gag	agg	aac	agc	aac	ctg	gtg	855
1	Met	Glu	Thr	Pro	Ser	Gln	Arg	Arg	Ala	Thr	Arg	Ser	Gly	Ala	Gln		15	271	Leu	Asp	Asn	Ala	Arg	Gln	Ser	Ala	Glu	Arg	Asn	Ser	Asn	Leu	Val	285
46	gcc	agc	tcc	act	cgg	ctg	tcg	ccc	acc	cgc	atc	acc	egg	ctg	cag		90	856	ggg	gct	gcc	cac	gag	gag	ctg	cag	cag	tcg	cgc	atc	cgc	atc	gac	900
16	Ala	Ser	Ser	Thr	Pro	Leu	Ser	Pro	Thr	Arg	Ile	Thr	Arg	Leu	Gln		30	286	Gly	Ala	Ala	His	Glu	Glu	Leu	Gln	Gln	Ser	Arg	Ile	Arg	Ile	Asp	300
91	gag	aag	gag	gac	ctg	cag	gag	ctc	aat	gat	cgc	ttg	gcg	gtc	tac		135	901	agc	ctc	tct	gcc	cag	ctc	agc	cag	ctc	cag	aag	cag	ctg	gca	gcc	945
31	Glu	Lys	Glu	Asp	Leu	Gln	Glu	Leu	Asn	Asp	Arg	Leu	Ala	Val	Tyr		45	301	Ser	Leu	Ser	Ala	Gln	Leu	Ser	Gln	Leu	Gln	Lys	Gln	Leu	Ala	Ala	315
136	atc	gac	cgt	gtg	cgc	tcg	ctg	gaa	acg	gag	aac	gca	ggg	ctg	cgc		180	946	aag	gag	gcg	aag	ctt	cga	gac	ctg	gag	gac	tca	ctg	gcc	cgt	gag	990
46	Ile	Asp	Arg	Val	Arg	Ser	Leu	Glu	Thr	Glu	Asn	Ala	Gly	Leu	Arg		60	316	Lys	Glu	Ala	Lys	Leu	Arg	Asp	Leu	Glu	Asp	Ser	Leu	Ala	Arg	Glu	330
181	ctt	cgc	atc	acc	gag	tct	gaa	gag	gtg	gtc	agc	cgc	gag	gtg	tcc		225	991	egg	gac	acc	agc	egg	egg	ctg	ctg	gcg	gaa	aag	gag	egg	gag	atg	1035
61	Thr	Leu	Ile	Thr	Glu	Val	Val	Ser	Arg	Glu	Val	Ser					75	331	Arg	Asp	Thr	Ser	Arg	Arg	Leu	Leu	Ala	Glu	Lys	Glu	Arg	Glu	Met	345
226	ggc	atc	aag	gcc	gcc	tac	gag	gcc	gag	ctc	ggg	gat	gcc	cgc	aag		270	1036	gcc	gag	atg	egg	gca	agg	atg	cag	cag	cag	ctg	gac	gag	tac	cag	1080
76	Gly	Ile	Lys	Ala	Ala	Tyr	Glu	Ala	Glu	Leu	Gly	Asp	Ala	Arg	Lys		90	346	Ala	Glu	Met	Arg	Ala	Arg	Met	Gln	Gln	Gln	Leu	Asp	Glu	Tyr	Gln	360
271	acc	ctt	gac	tca	gta	gcc	aag	gag	cgc	gcc	cgc	ctg	cag	ctg	gag		315	1081	gag	ctt	ctg	gac	atc	aag	ctg	gcc	ctg	gac	atg	gag	atc	cac	gcc	1125
91	Thr	Leu	Asp	Ser	Val	Ala	Lys	Glu	Arg	Ala	Arg	Leu	Gln	Leu	Glu		105	361	Glu	Leu	Leu	Asp	Ile	Lys	Leu	Ala	Leu	Asp	Met	Glu	Ile	His	Ala	375
316	ctg	agc	aaa	gtg	cgt	gag	gag	ttt	aag	gag	ctg	aaa	gcg	cgc	aat		360	1126	tac	cgc	aag	ctc	ttg	gag	ggc	gag	gag	agg	cta	cgc	ctg	tcc	1170	
106	Leu	Ser	Lys	Val	Arg	Glu	Glu	Phe	Lys	Glu	Leu	Lys	Ala	Arg	Asn		120	376	Tyr	Arg	Lys	Leu	Leu	Glu	Gly	Glu	Glu	Glu	Arg	Leu	Arg	Leu	Ser	390
361	acc	aag	aag	gag	ggg	gac	ctg	ata	gct	gct	cag	gct	egg	ctg	aag		405	1171	ccc	agc	cct	acc	tcg	cag	cgc	agc	cgt	ggc	cgt	gct	tcc	tct	cac	1215
121	Thr	Lys	Lys	Glu	Gly	Asp	Leu	Ile	Ala	Ala	Gln	Ala	Arg	Leu	Lys		135	391	Pro	Ser	Pro	Thr	Ser	Gln	Arg	Ser	Arg	Gly	Arg	Ala	Ser	Ser	His	405
406	gac	ctg	gag	gct	ctg	ctg	aac	tcc	aag	gag	gcc	gca	ctg	agc	act		450	1216	tca	tcc	cag	aca	cag	ggt	ggg	ggc	agc	gtc	acc	aaa	aag	cgc	aaa	1260
136	Asp	Glu	Glu	Ala	Leu	Leu	Asn	Ser	Lys	Glu	Ala	Ala	Leu	Ser	Thr		150	406	Ser	Ser	Gln	Thr	Gln	Gly	Gly	Gly	Ser	Val	Thr	Lys	Lys	Arg	Lys	420
451	gct	ctc	agt	gag	aag	cgc	acg	ctg	gag	ggc	gag	ctg	cat	gat	ctg		495	1261	ctg	gag	tcc	act	gag	agc	cgc	agc	ttc	tca	cag	cac	gca	cgc	1305	
151	Ala	Leu	Ser	Glu	Lys	Arg	Thr	Leu	Glu	Gly	Glu	Leu	His	Asp	Leu		165	421	Leu	Glu	Ser	Thr	Glu	Ser	Arg	Ser	Ser	Phe	Ser	Gln	His	Ala	Arg	435
496	cgg	ggc	cag	gtg	gcc	aag	ctt	gag	gca	gcc	cta	ggt	gag	gcc	aag		540	1306	act	agc	ggg	cgc	gtg	gcc	gtg	gag	gag	gtg	gat	gag	gag	ggc	aag	1350
166	Arg	Gly	Gln	Val	Ala	Lys	Leu	Glu	Ala	Ala	Leu	Gly	Glu	Ala	Lys		180	436	Thr	Ser	Gly	Arg	Val	Ala	Val	Glu	Glu	Val	Asp	Glu	Glu	Gly	Lys	450
541	aag	caa	ctt	cag	gat	gag	atg	ctg	cgg	cgg	gtg	gat	gct	gag	aac		585	1351	ttt	gtc	egg	ctg	cgc	aac	aag	tcc	aat	gag	gac	cag	tcc	atg	ggc	1395
181	Lys	Gln	Leu	Gln	Asp	Glu	Met	Leu	Arg	Arg	Val	Asp	Ala	Glu	Asn		195	451	Phe	Val	Arg	Leu	Arg	Asn	Lys	Ser	Asn	Glu	Asp	Gln	Ser	Met	Gly	465
586	agg	ctg	cag	acc	atg	aag	gag	gaa	ctg	gac	ttc	cag	aag	aac	atc		630	1396	aat	tgg	cag	atc	aag	cgc	cag	aat	gga	gat	gat	ccc	ttg	ctg	act	1440
196	Arg	Leu	Gln	Thr	Met	Lys	Glu	Glu	Leu	Asp	Phe	Gln	Lys	Asn	Ile		210	466	Asn	Trp	Gln	Ile	Lys	Arg	Gln	Asn	Gly	Asp	Asp	Pro	Leu	Leu	Thr	480
631	tac	agt	gag	gag	ctg	cgt	gag	acc	aag	cgc	cgt	cat	gag	acc	cga		675	1441	tac	cgg	ttc	cca	cca	aag	ttc	acc	ctg	aag	gct	ggg	cag	gtg	gtg	1485
211	Tyr	Ser	Glu	Glu	Leu	Arg	Glu	Thr	Lys	Arg	Arg	His	Glu	Thr	Arg		720	481	Tyr	Arg	Phe	Pro	Pro	Lys	Phe	Thr	Leu	Lys	Ala	Gly	Gln	Val	Val	495
676	ctg	gtg	gag	att	gac	aat	ggg	aag	cag	cgt	gag	ttt	gag	agc	egg		725	1486	acg	atc	tgg	gct	gca	gga	gct	ggg	gcc	acc	cac	agc	ccc	cct	acc	1530
226	Leu	Val	Glu	Ile	Asp	Asn	Gly	Lys	Gln	Arg	Glu	Phe	Glu	Ser	Arg		240	496	Thr	Ile	Trp	Ala	Ala	Gly	Ala	Gly	Ala	Thr	His	Ser	Pro	Pro	Thr	510
721	ctg	gcg	gat	gcg	ctg	cag	gaa	ctg	cgg	gcc	cag	cat	gag	gac	cag		765	1531	gac	ctg	gtg	tgg	aag	gca	cag	aac	acc	tgg	ggc	tgc	ggg	aac	agc	1575
241	Leu	Ala	Asp	Ala	Leu	Gln	Glu	Leu	Arg	Ala	Gln	His	Glu	Asp	Gln		255	511	Asp	Leu	Val	Trp	Lys	Ala	Gln	Asn	Thr	Trp	Gly	Cys	Gly	Asn	Ser	525
766	gtg	gag	cag	tat	aag	aag	gag	ctg	gag	aag	act	tat	tct	gcc	aag		810	1576	ctg	cgt	acg	gct	ctc	atc	aac	tcc	act	ggg	gaa	gaa	gtg	gcc	atg	1620
256	Val	Glu	Gln	Tyr	Lys	Lys	Glu	Leu	Glu	Lys	Thr	Tyr	Ser	Ala	Lys		270	526	Leu	Arg	Thr	Ala	Leu	Ile	Asn	Ser	Thr	Gly	Glu	Glu	Val	Ala	Met	540

Yellow: Start codon

Blue: Frameshift mutation site due to deletion

Red: Stop codon

B Translation of *LMNA* T518 frameshit mutation transcript

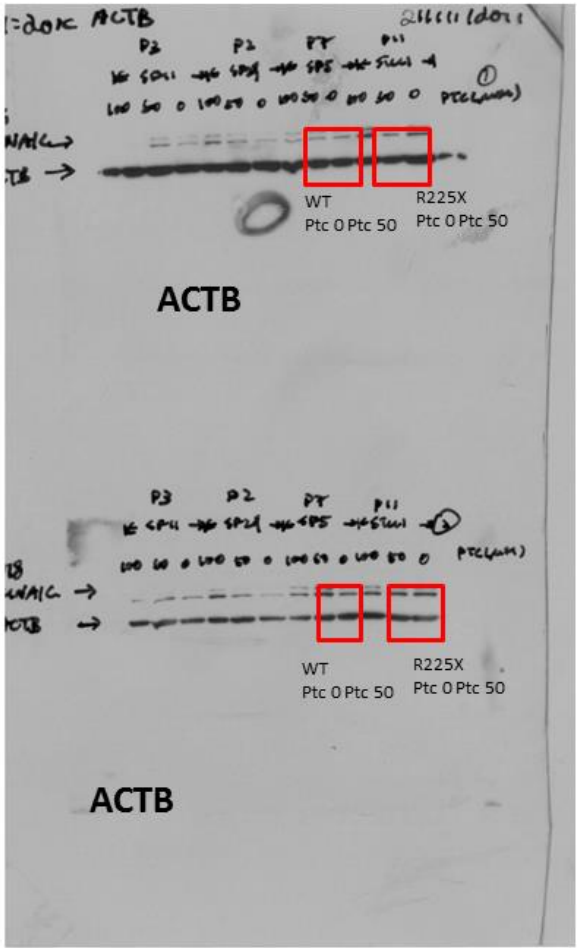
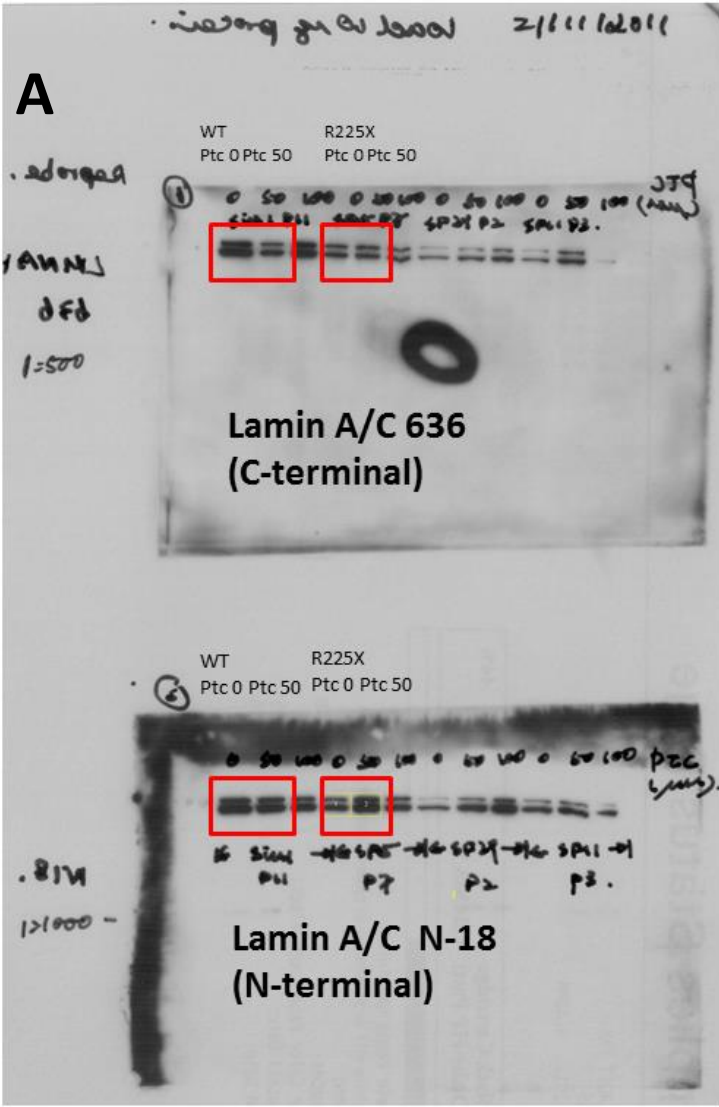
1	atg	gag	acc	ccg	tcc	cag	cgg	cgc	gcc	acc	cgc	agc	ggg	gcg	cag	45	856	ggg	gct	gcc	cac	gag	gag	ctg	cag	cag	tcg	cgc	atc	cgc	atc	gac	900	
1	Met	Glu	Thr	Pro	Ser	Gln	Arg	Arg	Ala	Thr	Arg	Ser	Gly	Ala	Gln	15	286	Gly	Ala	Ala	His	Glu	Glu	Leu	Gln	Gln	Ser	Arg	Ile	Arg	Ile	Asp	300	
46	gcc	agc	tcc	act	ccg	ctg	tcg	ccc	acc	cgc	atc	acc	cgg	ctg	cag	90	901	agc	ctc	tct	gcc	cag	ctc	agc	cag	ctc	cag	aag	cag	ctg	gca	gcc	945	
16	Ala	Ser	Ser	Thr	Pro	Leu	Ser	Pro	Thr	Arg	Ile	Thr	Arg	Leu	Gln	30	301	Ser	Leu	Ser	Ala	Gln	Leu	Ser	Gln	Leu	Gln	Lys	Gln	Leu	Ala	Ala	315	
91	gag	aag	gag	gac	ctg	cag	gag	ctc	aat	gat	cgc	ttg	gcg	gtc	tac	135	946	aag	gag	gcg	aag	ctt	cga	gac	ctg	gag	gac	tca	ctg	gcc	cgt	gag	990	
31	Glu	Lys	Glu	Asp	Leu	Gln	Glu	Leu	Asn	Asp	Arg	Leu	Ala	Val	Tyr	45	316	Lys	Glu	Ala	Lys	Leu	Arg	Asp	Leu	Glu	Asp	Ser	Leu	Ala	Arg	Glu	330	
136	atc	gac	cgt	gtg	cgc	tcg	ctg	gaa	acg	gag	aac	gca	ggg	ctg	cgc	180	991	cgg	gac	acc	agc	cgg	cgg	ctg	ctg	gcg	gaa	aag	gag	cgg	gag	atg	1035	
46	Ile	Asp	Arg	Val	Arg	Ser	Leu	Glu	Thr	Glu	Asn	Ala	Gly	Leu	Arg	60	331	Arg	Asp	Thr	Ser	Arg	Arg	Leu	Leu	Ala	Glu	Lys	Glu	Arg	Glu	Met	345	
181	ctt	cgc	atc	acc	gag	tct	gaa	gag	gtg	gtc	agc	cgc	gag	gtg	tcc	225	1036	gcc	gag	atg	cgg	gca	agg	atg	cag	cag	cag	ctg	gac	gag	tac	cag	1080	
61	Leu	Arg	Ile	Thr	Glu	Ser	Glu	Glu	Val	Val	Ser	Arg	Glu	Val	Ser	75	346	Ala	Glu	Met	Arg	Ala	Arg	Met	Gln	Gln	Leu	Asp	Glu	Tyr	Gln	360		
226	ggc	atc	aag	gcc	gcc	tac	gag	gcc	gag	ctc	ggg	gat	gcc	cgc	aag	270	1081	gag	ctt	ctg	gac	atc	aag	ctg	gcc	ctg	gac	atg	gag	atc	cac	gcc	1125	
76	Gly	Ile	Lys	Ala	Ala	Tyr	Glu	Ala	Glu	Leu	Gly	Asp	Ala	Arg	Lys	90	361	Glu	Leu	Leu	Asp	Ile	Lys	Leu	Ala	Leu	Asp	Met	Glu	Ile	His	Ala	375	
271	acc	ctt	gac	tca	gta	gcc	aag	gag	cgc	gcc	cgc	ctg	cag	ctg	gag	315	1126	tac	cgc	aag	ctc	ttg	gag	ggc	gag	gag	gag	agg	cta	cgc	ctg	tcc	1170	
91	Thr	Leu	Asp	Ser	Val	Ala	Lys	Glu	Arg	Ala	Arg	Leu	Gln	Leu	Glu	105	376	Tyr	Arg	Lys	Leu	Leu	Glu	Gly	Glu	Glu	Glu	Arg	Leu	Arg	Leu	Ser	390	
316	ctg	agc	aaa	gtg	cgt	gag	gag	ttt	aag	gag	ctg	aaa	gcg	cgc	aat	360	1171	ccc	agc	cct	acc	tcg	cag	cgc	agc	cgt	ggc	cgt	gct	tcc	tct	cac	1215	
106	Leu	Ser	Lys	Val	Arg	Glu	Glu	Phe	Lys	Glu	Leu	Lys	Ala	Arg	Asn	120	391	Pro	Ser	Pro	Thr	Ser	Gln	Arg	Ser	Arg	Gly	Arg	Ala	Ser	Ser	His	405	
361	acc	aag	aag	gag	ggt	gac	ctg	ata	gct	gct	cag	gct	cgg	ctg	aag	405	1216	tca	tcc	cag	aca	cag	ggt	ggg	ggc	agc	gtc	acc	aaa	aag	cgc	aaa	1260	
121	Thr	Lys	Lys	Glu	Gly	Asp	Leu	Ile	Ala	Ala	Gln	Ala	Arg	Leu	Lys	135	406	Ser	Ser	Gln	Thr	Gln	Gly	Gly	Gly	Ser	Val	Thr	Lys	Lys	Arg	Lys	420	
406	gac	ctg	gag	gct	ctg	ctg	aac	tcc	aag	gag	gcc	gca	ctg	agc	act	450	1261	ctg	gag	tcc	act	gag	agc	cgc	agc	agc	ttc	tca	cag	cac	gca	cgc	1305	
136	Asp	Leu	Glu	Ala	Leu	Leu	Asn	Ser	Lys	Glu	Ala	Ala	Leu	Ser	Thr	150	421	Leu	Glu	Ser	Thr	Glu	Ser	Arg	Ser	Ser	Phe	Ser	Gln	His	Ala	Arg	435	
451	gct	ctc	agt	gag	aag	cgc	acg	ctg	gag	ggc	gag	ctg	cat	gat	ctg	495	1306	act	agc	ggg	cgc	gtg	gcc	gtg	gag	gag	gtg	gat	gag	gag	ggc	aag	1350	
151	Ala	Leu	Ser	Glu	Lys	Arg	Thr	Leu	Glu	Gly	Glu	Leu	His	Asp	Leu	165	436	Thr	Ser	Gly	Arg	Val	Ala	Val	Glu	Glu	Val	Asp	Glu	Glu	Gly	Lys	450	
496	cgg	ggc	cag	gtg	gcc	aag	ctt	gag	gca	gcc	cta	ggt	gag	gcc	aag	540	1351	ttt	gtc	cgg	ctg	cgc	aac	aag	tcc	aat	gag	gac	cag	tcc	atg	ggc	1395	
166	Arg	Gly	Gln	Val	Ala	Lys	Leu	Glu	Ala	Ala	Leu	Gly	Glu	Ala	Lys	180	451	Phe	Val	Arg	Leu	Arg	Asn	Lys	Ser	Asn	Glu	Asp	Gln	Ser	Met	Gly	465	
541	aag	caa	ctt	cag	gat	gag	atg	ctg	cgg	cgg	gtg	gat	gct	gag	aac	585	1396	aat	tgg	cag	atc	aag	cgc	cag	aat	gga	gat	gat	ccc	ttg	ctg	act	1440	
181	Lys	Gln	Leu	Gln	Asp	Glu	Met	Leu	Arg	Arg	Val	Asp	Ala	Glu	Asn	195	466	Asn	Trp	Gln	Ile	Lys	Arg	Gln	Asn	Gly	Asp	Asp	Pro	Leu	Leu	Thr	480	
586	agg	ctg	cag	acc	atg	aag	gag	gaa	ctg	gac	ttc	cag	aag	aac	atc	630	1441	tac	cgg	ttc	cca	cca	aag	ttc	acc	ctg	aag	gct	ggg	cag	gtg	gtg	1485	
196	Arg	Leu	Gln	Thr	Met	Lys	Glu	Glu	Leu	Asp	Phe	Gln	Lys	Asn	Ile	210	481	Tyr	Arg	Phe	Pro	Pro	Lys	Phe	Thr	Leu	Lys	Ala	Gly	Gln	Val	Val	495	
631	tac	agt	gag	gag	ctg	cgt	gag	acc	aag	cgc	cgt	cat	gag	acc	cga	675	1486	acg	atc	tgg	gct	gca	gga	gct	ggg	gcc	acc	cac	agc	ccc	cct	acc	1530	
211	Tyr	Ser	Glu	Glu	Leu	Arg	Glu	Thr	Lys	Arg	Arg	His	Glu	Thr	Arg	225	496	Thr	Ile	Trp	Ala	Ala	Gly	Ala	Gly	Ala	Thr	His	Ser	Pro	Pro	Thr	510	
676	ctg	gtg	gag	att	gac	aat	ggg	aag	cag	cgt	gag	ttt	gag	agc	cgg	720	1531	gac	ctg	gtg	tgg	aag	gca	cag	aac	act	ggg	gct	gcg	gga	aca	gcc	1575	
226	Leu	Val	Glu	Ile	Asp	Asn	Gly	Lys	Gln	Arg	Glu	Phe	Glu	Ser	Arg	240	511	Asp	Leu	Val	Trp	Lys	Ala	Gln	Asn	Thr	Gly	Ala	Ala	Gly	Thr	Ala	525	
721	ctg	gcg	gat	gcg	ctg	cag	gaa	ctg	cgg	gcc	cag	cat	gag	gac	cag	765	1577	tgc	gta	cgg	ctc	tca	tca	act	cca	ctg	ggg	aag	aag	tgg	cca	tgc	1621	
241	Leu	Ala	Asp	Ala	Leu	Gln	Glu	Leu	Arg	Ala	Gln	His	Glu	Asp	Gln	255	526	Cys	Val	Arg	Leu	Ser	Ser	Thr	Pro	Leu	Gly	Lys	Lys	Trp	Pro	Cys	540	
766	gtg	gag	cag	tat	aag	aag	gag	ctg	gag	aag	act	tat	tct	gcc	aag	810	1622	aca	aac	taa	tac	act	caa	Ter	cta	taa	tta	aaa	aca	aca	aaa	ata	1666	
256	Val	Glu	Gln	Tyr	Lys	Lys	Thr	Leu	Glu	Lys	Thr	Tyr	Ser	Ala	Lys	270																		
811	ctg	gac	aat	gcc	agg	cag	tct	gct	gag	agg	aac	agc	aac	ctg	gtg	855	541	Ala	Ser	Trp	Cys	Ala	Gln	End	Leu	Trp	Leu	Arg	Thr	Thr	Arg	Met	555	
271	Leu	Asp	Asn	Ala	Arg	Gln	Ser	Ala	Glu	Arg	Asn	Ser	Asn	Leu	Val	285																		

↑
Premature stop codon

Yellow: Start codon

Blue: Frameshift mutation site due to deletion

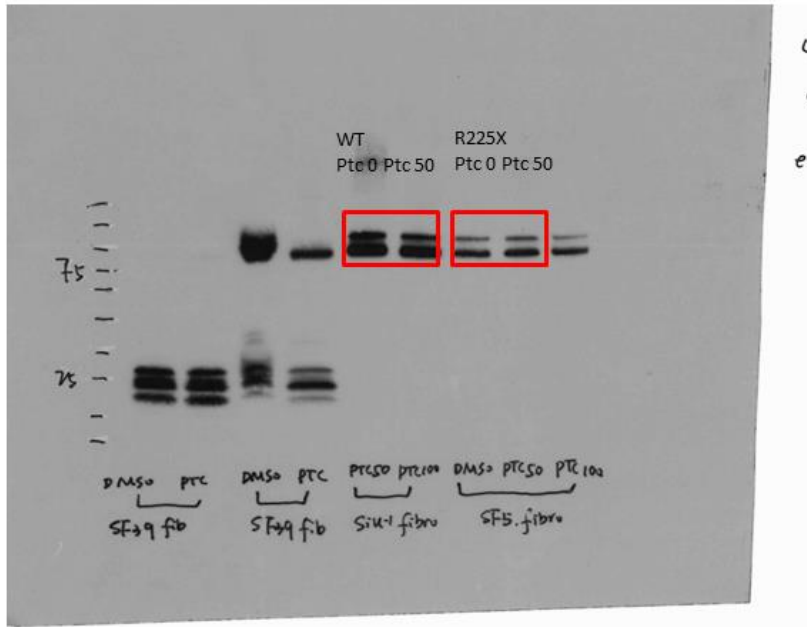
Red: Stop codon



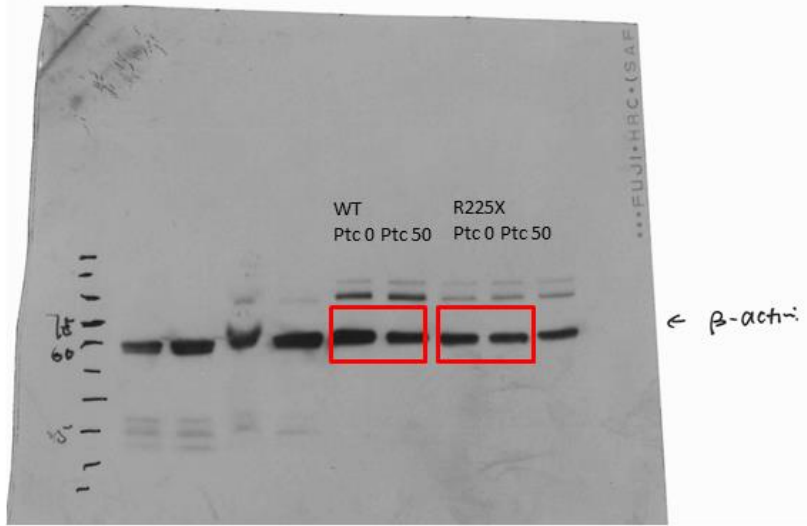
Skin fibroblast
21/11/2011

Figure S2. A.

B

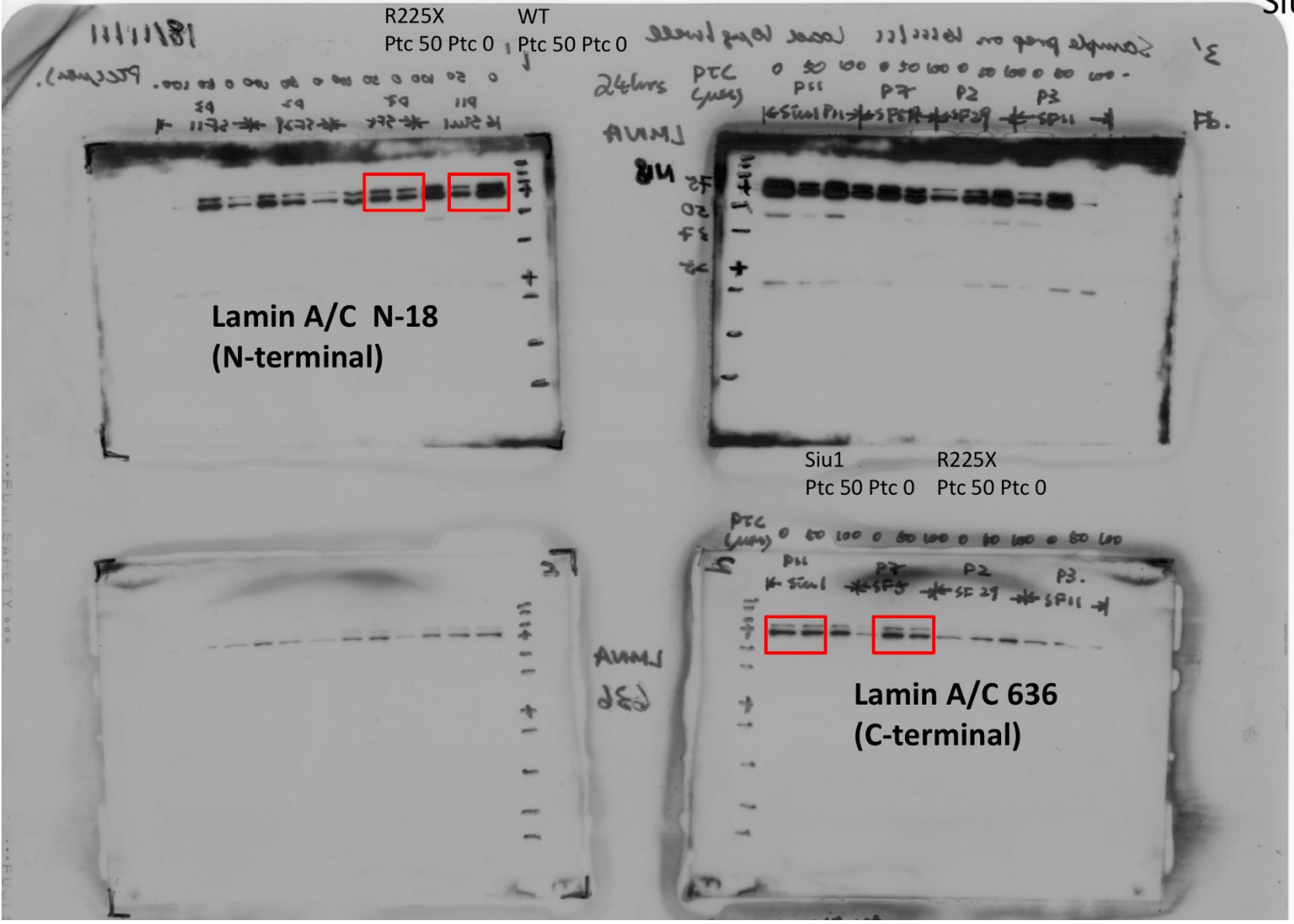


Skin fibroblast
6/12/2016
SF5: R225X;
Siu-1: WT

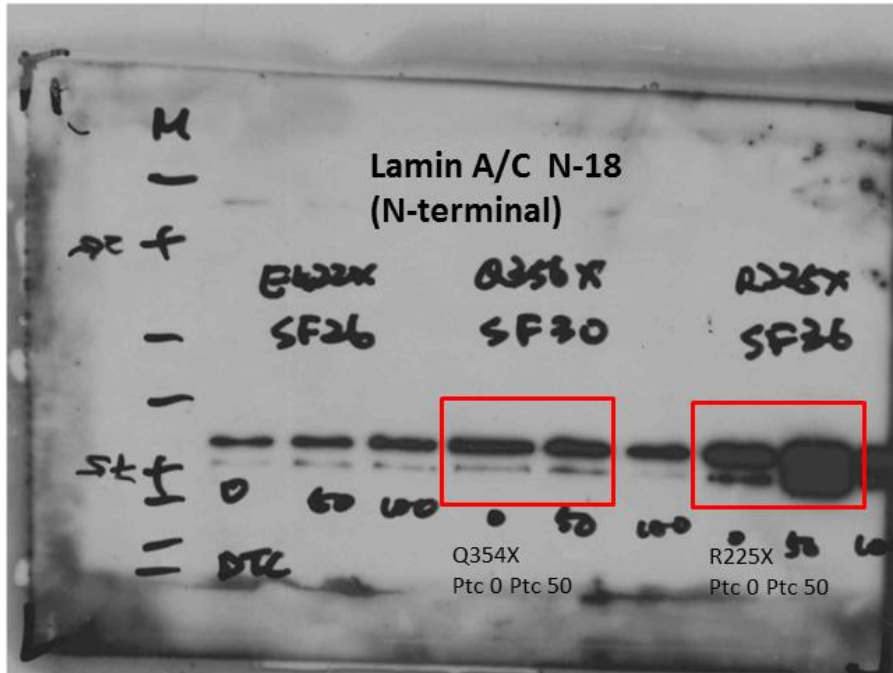


Skin fibroblast
SF5: R225X;
Siu-1: WT

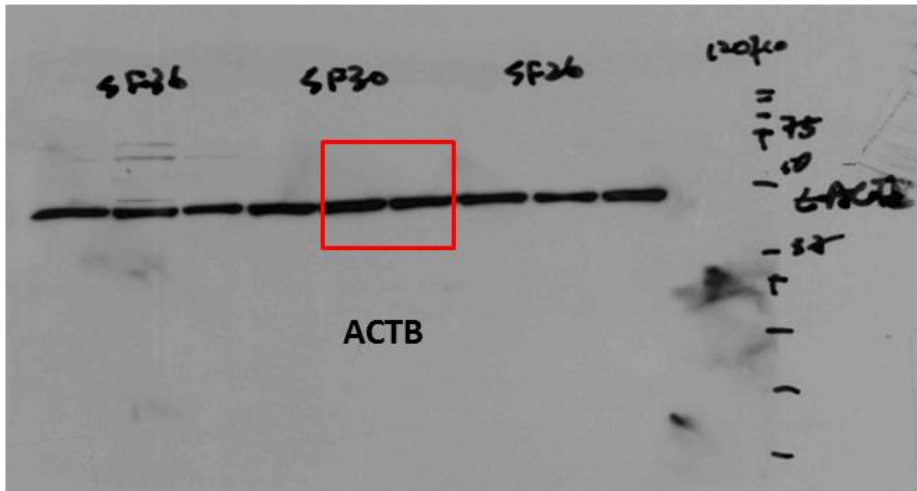
C



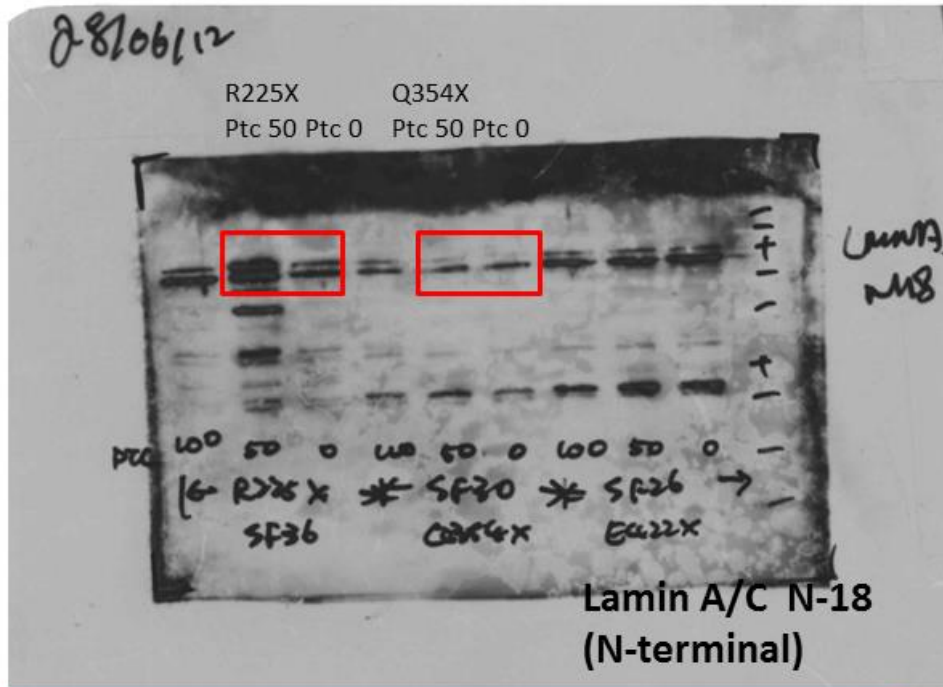
D



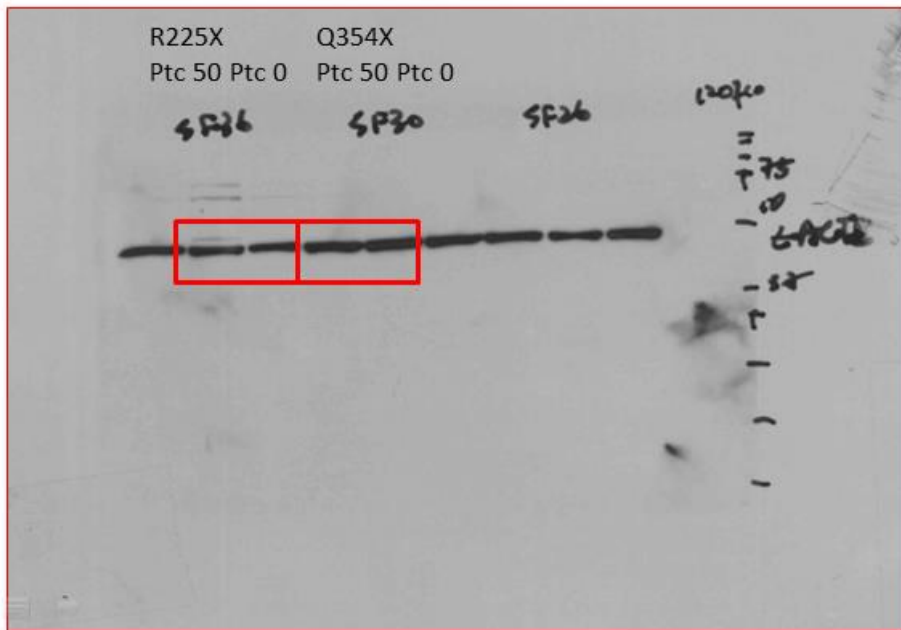
Skin fibroblast
19/6/12
sf30 = Q354X



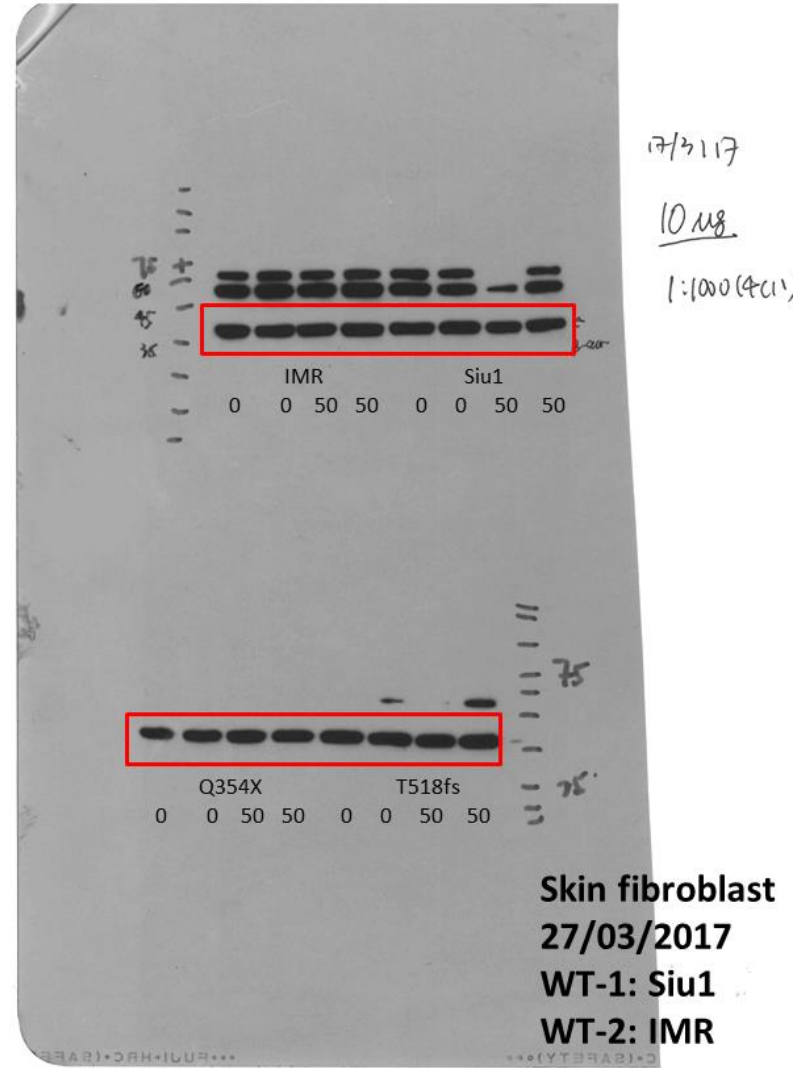
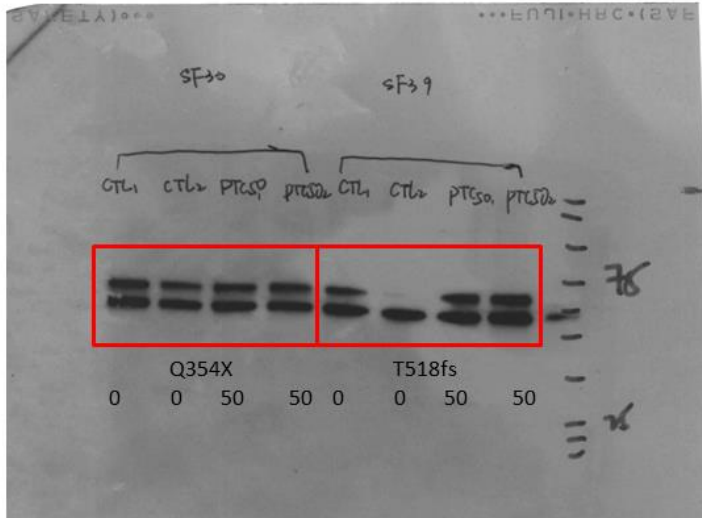
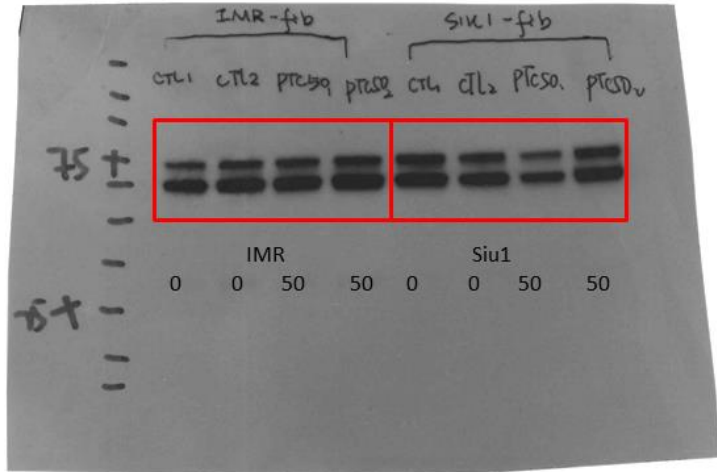
E



Skin fibroblast
SF36: R225X
SF30: Q354X

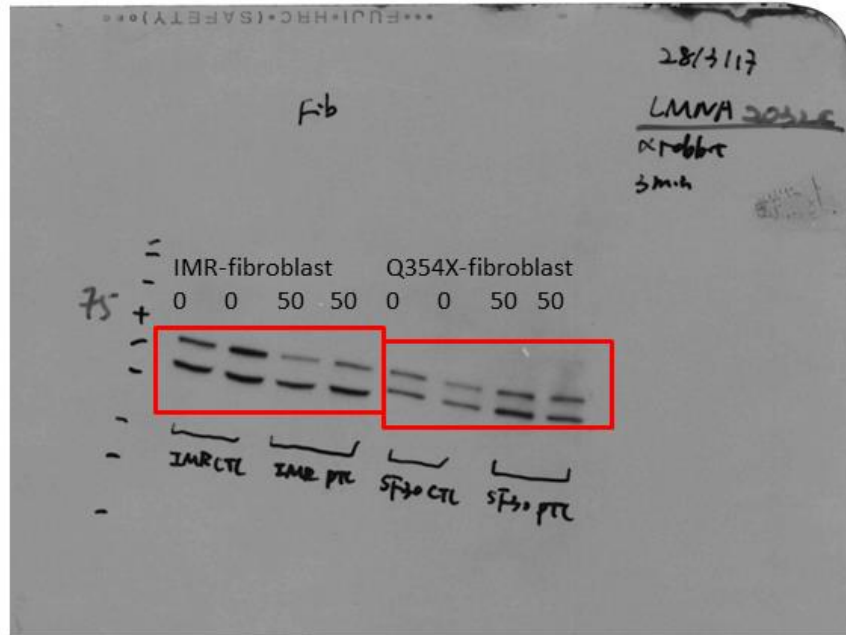


F

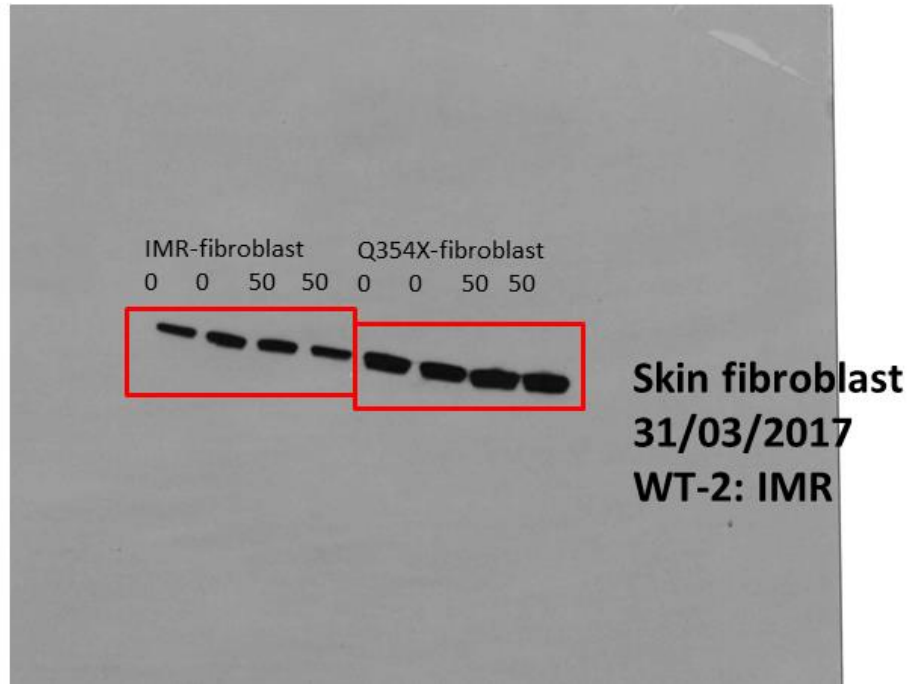


G

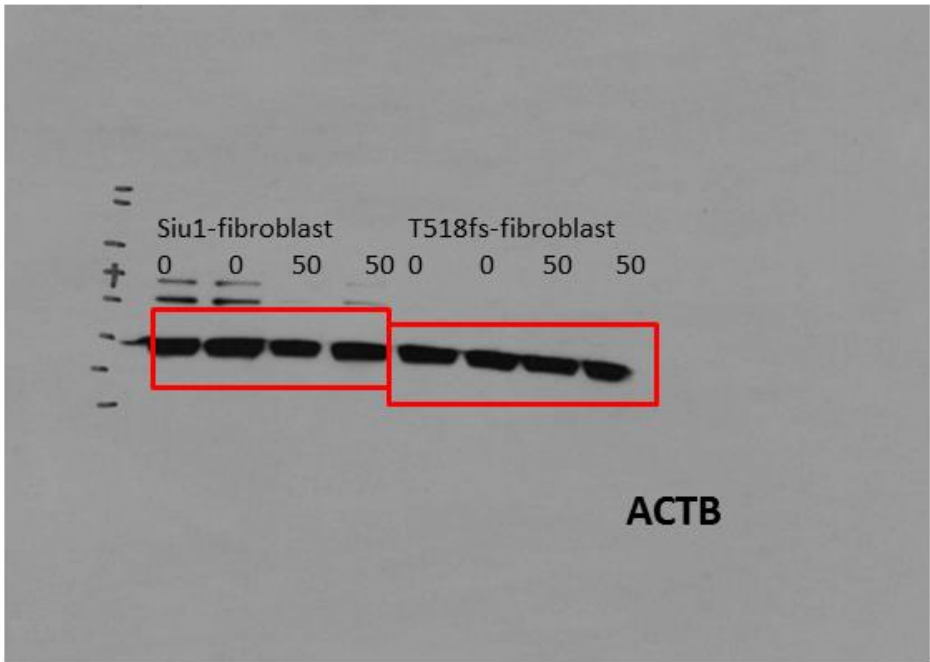
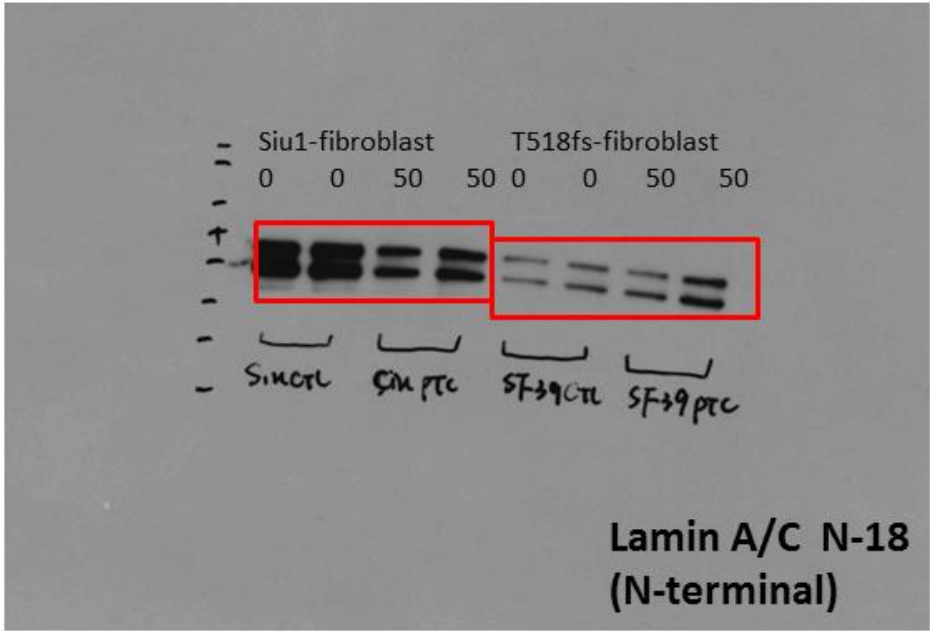
Lamin A/C N-18
(N-terminal)



ACTB



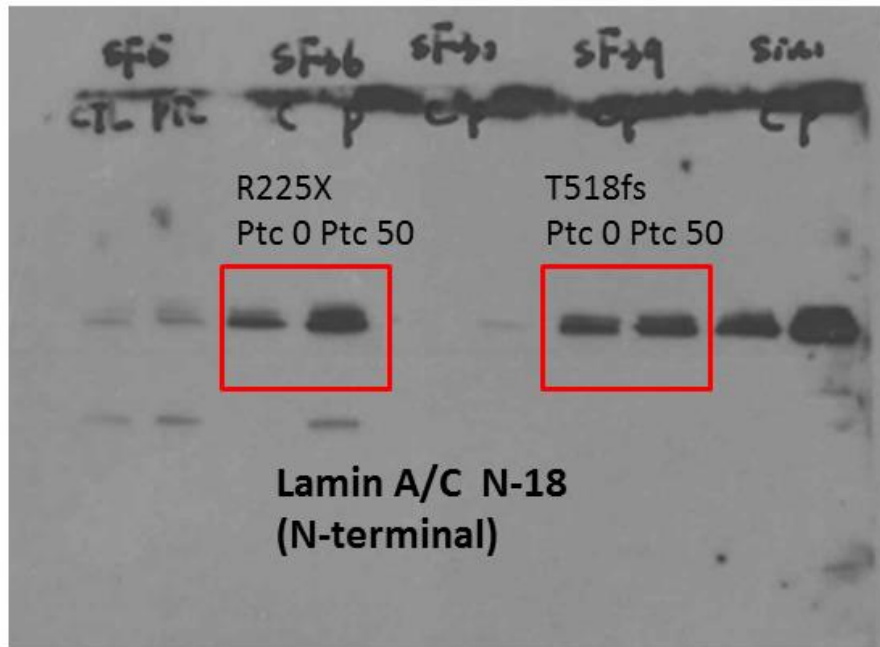
H



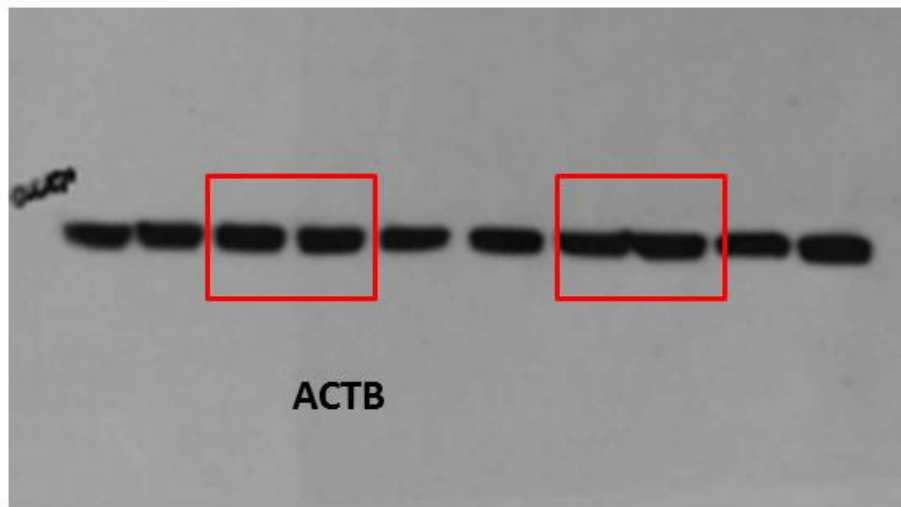
Skin fibroblast
27/03/2017
WT-2: IMR

I

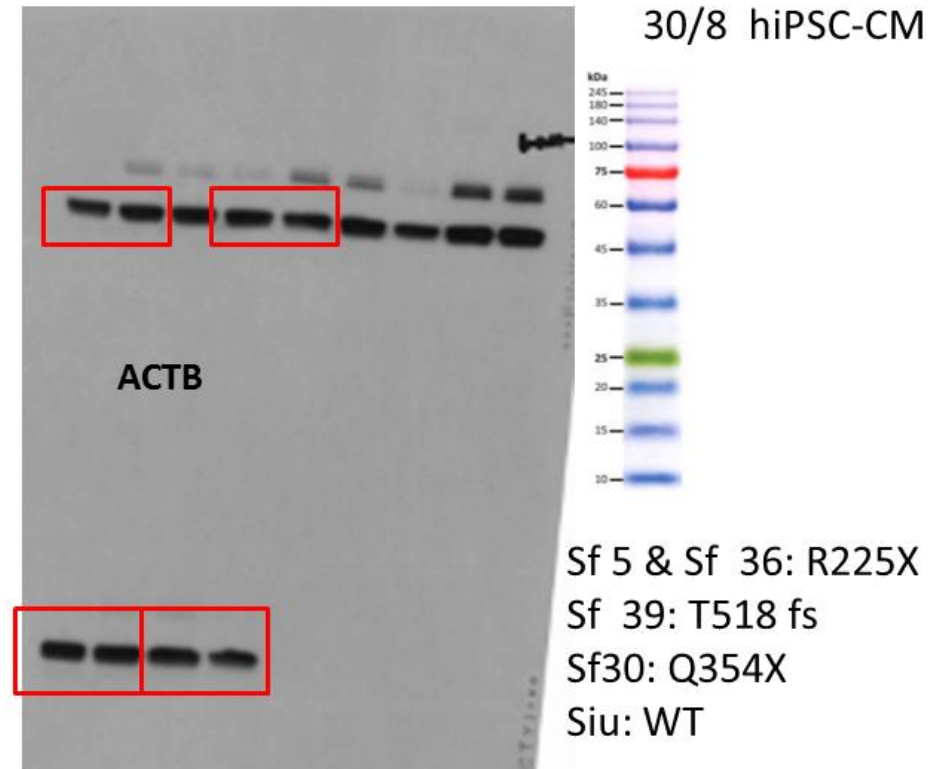
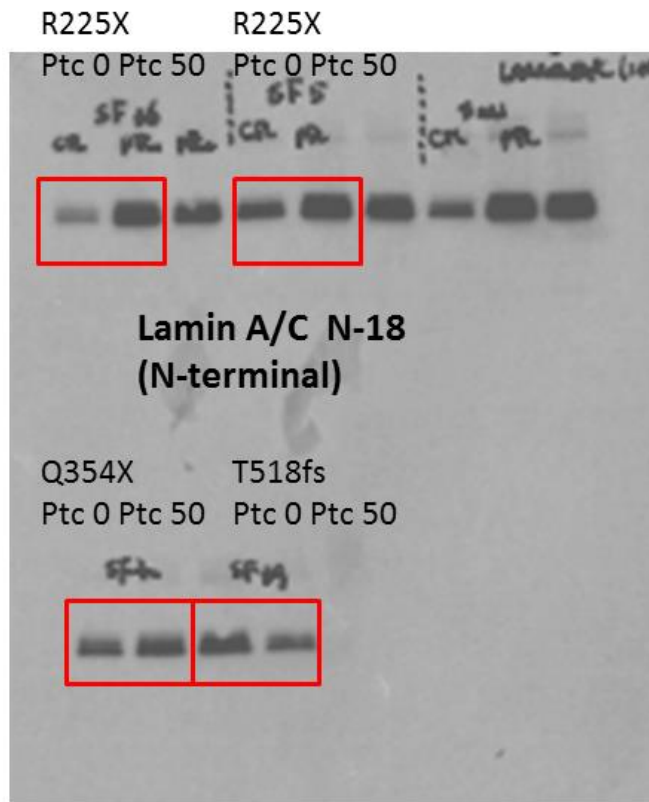
19/8 hiPSC-CM



Sf 36 = Q354X
Sf 39 = T518fs

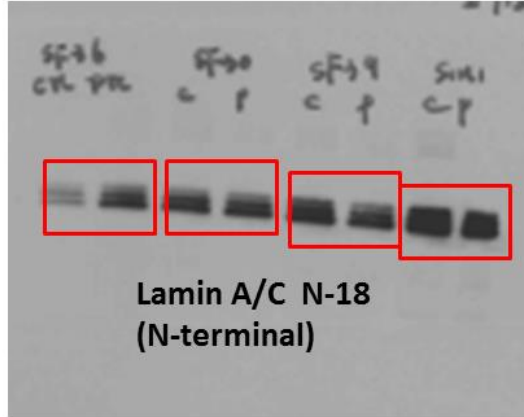


J

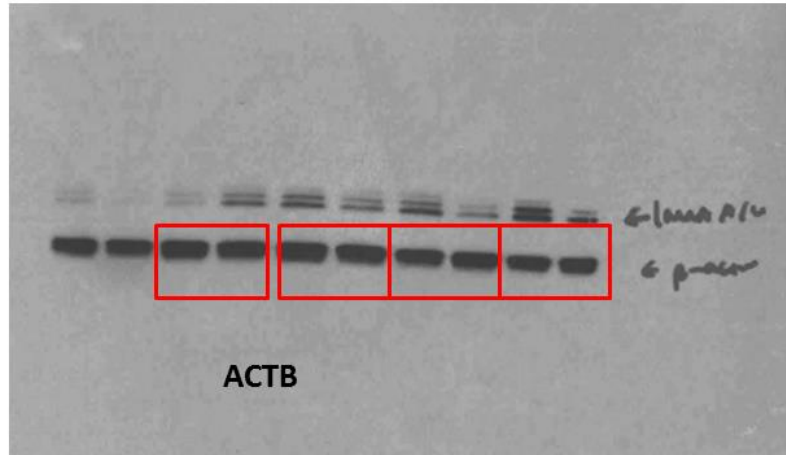


K

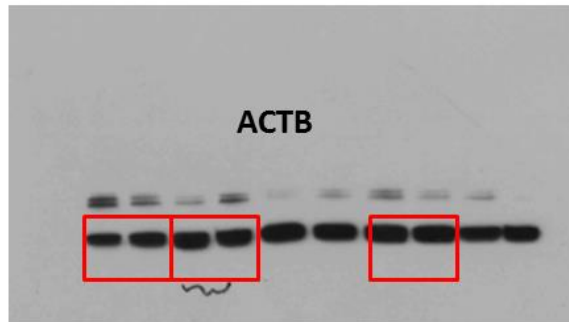
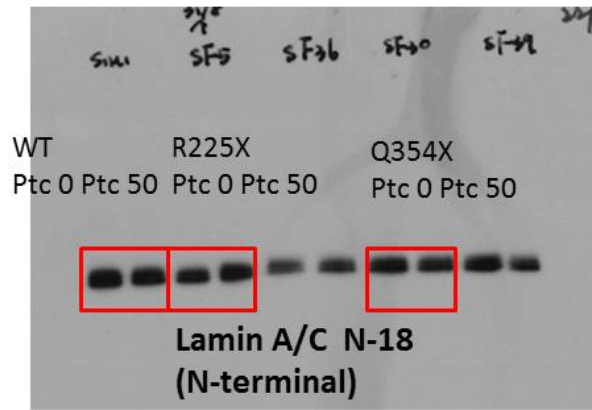
R225X Q354X T518fs Siu1
Ptc 0 Ptc 50 Ptc 0 Ptc 50 Ptc 0 Ptc 50 Ptc 0 Ptc 50



6/9 hiPSC-CM
Wt
Sf36 = R225X
Sf30 = Q354X
Sf39 = T518fs



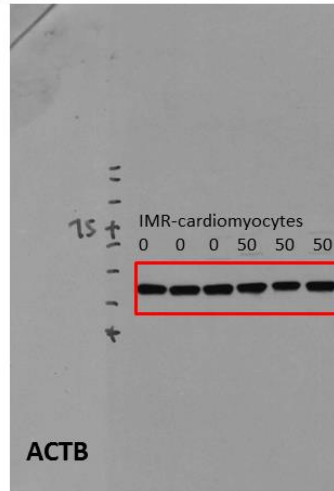
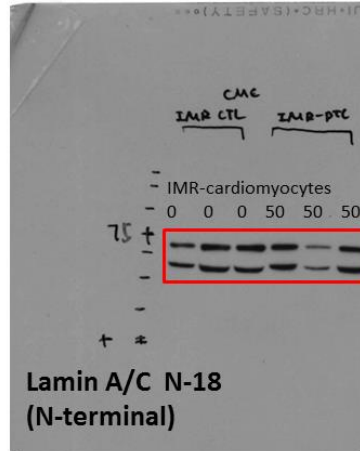
L



22/9 hiPSC-CM
Siu1: WT
SF5-R225X
SF30-Q354X



M



hiPSC-CM
31/03/2017
WT-2: IMR

Supplemental Figure Legends:

Figure S1. Translational product of *LMNA* T518fs mutated transcript. (A) Wild type *LMNA* mRNA transcript (NM_170707); (B) Prediction of second open reading frame (ORF) with one “c” deletion at the 1554th codon position in the *LMNA* mRNA transcript, the premature stop codon with sequence of “TGA” will be generated at an earlier position at the 547th amino acid, shortening of the Lmna protein that is supposed to be transcribed (reduced from the 665th to 547th amino acids). Moreover, even after PTC124 read-through, the amino acid sequence after frameshift mutation (the 519th amino acid) would be totally deviated from the native lamin A/C ones.

Figure S2. Effects of PTC124 on the expression of lamin A/C proteins in dermal fibroblasts (A-H) and hiPSC-derived cardiomyocytes (hiPSC-CMC) (I-M) derived from wild-type (*LMNA*^{WT1/WT1} & *LMNA*^{WT2/WT2}) and *LMNA* mutants (*LMNA*^{R225X/WT}, *LMNA*^{Q354X/WT} and *LMNA*^{T518fs/WT}). Original images of immunoblots with at least one wild type sample loaded on the same gel with patient samples. Lamin A/C (clone N18) were probed with antibody that recognized N-terminal, while beta-actin (ACTB) was used as the internal control for normalization of protein loading. Three to six independent samples were prepared for western blot analysis.

Modeling Treatment Response for Lamin A/C Related Dilated Cardiomyopathy in Human Induced Pluripotent Stem Cells

Yee-Ki Lee, Yee-Man Lau, Zhu-Jun Cai, Wing-Hon Lai, Lai-Yung Wong, Hung-Fat Tse, Kwong-Man Ng and Chung-Wah Siu

J Am Heart Assoc. 2017;6:e005677; originally published July 28, 2017;

doi: 10.1161/JAHA.117.005677

The *Journal of the American Heart Association* is published by the American Heart Association, 7272 Greenville Avenue, Dallas, TX 75231
Online ISSN: 2047-9980

The online version of this article, along with updated information and services, is located on the World Wide Web at:

<http://jaha.ahajournals.org/content/6/8/e005677>